

1
2003
54814763



This is to certify that the
thesis entitled


NUMERICAL APPROACHES TO PREDICT BUBBLE
GROWTH IN VISCOUS LIQUIDS USING POLYNOMIAL
PROFILES

presented by

PRAVEEN K VASAM

has been accepted towards fulfillment
of the requirements for the

 M.S. degree in Mechanical Engineering



Major Professor's Signature

 8/18/2003

Date

PLACE IN RETURN BOX to remove this checkout from your record.
TO AVOID FINES return on or before date due.
MAY BE RECALLED with earlier due date if requested.

DATE DUE	DATE DUE	DATE DUE

**NUMERICAL APPROACHES TO PREDICT BUBBLE GROWTH IN
VISCOUS LIQUIDS USING POLYNOMIAL PROFILES**

By

Praveen K Vasam

A THESIS

**Submitted to
Michigan State University
In partial fulfillment of the requirements
for the degree of**

MASTER OF SCIENCE

Department of Mechanical Engineering

2003

ABSTRACT

NUMERICAL APPROACHES TO PREDICT BUBBLE GROWTH IN VISCOUS LIQUIDS USING POLYNOMIAL PROFILES

By

Praveen K Vasam

Modeling the phenomenon of bubble growth in liquids is important to fields such as boiling, cavitation, bubble removal during glass making, micro-gravity studies, composite materials, manufacturing void-free high performance materials, measuring the elongational viscosity and polymer processing. The main objective of this thesis is to develop improved models to predict bubble growth in a liquid shell using the previously developed models based on approximate polynomial profiles. Earlier models concentrated on obtaining solutions for growth of a bubble surrounded by an infinite amount of liquid. These models do not represent the correct physics of the problem as the bubbles are in fact surrounded by a finite shell of liquid and there is a finite amount of gas dissolved in the liquid. To incorporate the correct physics in the problem the new models are developed. In these new models the previously used numerical technique of 'Integral method' was retained. This method allows us to formulate approximate solutions for bubble growth. Since the polynomial profiles approximations give reasonable results during initial times, they were retained to develop a better solution for the bubble growth. The new models developed were solved and compared with the approximate solutions for bubble growth in an infinite medium and also the solutions obtained by solving the full diffusion equation. After comparing the results it was found that the new models predict the bubble growth behavior reasonably well.

Dedicated to my parents

ACKNOWLEDGEMENT

I am grateful to my thesis advisor Dr. Andre Benard for his valuable academic and non-academic assistance, continuous guidance, and motivation. He helped me a great deal in the formulations discussed in this work. His support and encouragement were crucial to the completion of this work. The constructive suggestions that he made during the reading of the manuscript of this thesis helped in improving it a great deal.

I would like to thank Dr. Indrek Wichman for the suggestions he made during the course of my research work. I want to acknowledge Dr. Craig Somerton's and Dr. Indrek Wichman's help for serving on my thesis defense committee.

I would like to thank all my instructors at Michigan State University (MSU) and Indian Institute of Technology (IIT), Madras who taught and encouraged me to reach this point. I would like to recognize the support and encouragement provided by my friends. Finally, a very special thanks to my parents and sisters for their love and moral support.

TABLE OF CONTENTS

LIST OF TABLES.....	vii
LIST OF FIGURES.....	viii
CHAPTER 1	1
INTRODUCTION	1
Issues.....	2
Motivation.....	4
CHAPTER 2	5
LITERATURE REVIEW	5
Bubble Nucleation in Liquids	5
Bubble Growth in Inviscid liquids.....	6
Bubble Growth in Viscous liquids.....	8
Summary.....	10
CHAPTER 3	12
THEORY OF SINGLE BUBBLE GROWTH.....	12
Growth of a Bubble in an Infinite Newtonian Medium.....	12
Hydrodynamics of the growth process	13
Mass diffusion.....	17
Integral method.....	19
Summary.....	25
CHAPTER 4	26
GROWTH OF A GAS BUBBLE IN A LIMITED BODY OF NEWTONIAN LIQUID	26
Hydrodynamics of the growth in a shell of Newtonian liquid.....	27
Diffusion of mass in the liquid shell	29
First approach.....	31
Alternate simplification	36
Second approach	37
Third approach	40
Complete solution	41
Numerical evaluation	44
Equilibrium calculations	46
Comparison of profiles	47

CHAPTER 5	59
SUMMARY AND CONCLUSIONS	59
Further Study	62
APPENDIX A.....	64
DERIVATION OF INTEGRAL DIFFUSION EQUATION	64
APPENDIX B	66
MATHEMATICA FILE.....	66
REFERENCES	70

LIST OF TABLES

Table 3.1: Expressions for the constants C_2 , C_3 , C_4 , C_5 , C_6 and C_7	25
Table 4.1: Methods adopted to predict bubble growth behavior in finite shell	32
Table 4.2: Lower and upper bounds for dimensionless variables C_2 , C_3 and C_4	45

LIST OF FIGURES

Figure 4.1: Schematic of a bubble in a shell of viscous liquid containing dissolved gas .	28
Figure 4.2: Comparison between various methods of evaluating the radius profiles for low thickness shell ($C_2 = 10^4$), $C_3 = 0.4$, $C_4 = 10^2$ (average gas diffusivity) and initial gas pressure $P_{g0}^* = 10$.	50
Figure 4.3: Comparison between approximate and accurate numerical solutions for medium thickness shell ($C_2 = 10^6$), $C_3 = 0.4$, $C_4 = 10^2$ (average gas diffusivity) and $P_{g0}^* = 10$.	51
Figure 4.4: Comparison between approximate and accurate numerical solutions for high thickness shell ($C_2 = 10^8$), $C_3 = 0.4$, $C_4 = 10^2$ (average gas diffusivity) and $P_{g0}^* = 10$.	52
Figure 4.5: Comparison between second, third order profile solutions using 'method 1' and the complete solution obtained by Arefmanesh [1] for medium thickness shell ($C_2 = 10^6$), $C_3 = 0.4$, $C_4 = 10$ (average gas diffusivity) and initial gas pressure $P_{g0}^* = 10$.	53
Figure 4.6: Comparison between second order, third order polynomial profile solutions for infinite medium and complete solution obtained by Arefmanesh [1] for medium thickness shell ($C_2 = 10^6$), $C_3 = 0.4$, $C_4 = 10$ (average gas diffusivity) and initial gas pressure $P_{g0}^* = 10$.	54
Figure 4.7: Comparison between approximate and accurate numerical solutions for medium thickness shell ($C_2 = 10^6$), $C_3 = 0.4$, $C_4 = 10^4$ (High gas diffusivity) and initial gas pressure $P_{g0}^* = 10$.	55
Figure 4.8: Comparison between various methods of evaluating the radius profiles for medium thickness shell ($C_2 = 10^6$), $C_3 = 0.4$, $C_4 = 10$ (low gas diffusivity) and initial gas pressure $P_{g0}^* = 10$.	56
Figure 4.9: Comparison between approximate and accurate numerical solutions for medium thickness shell ($C_2 = 10^6$), $C_3 = 0.4$, $C_4 = 10^2$ (average gas diffusivity) and low initial gas pressure $P_{g0}^* = 5$.	57
Figure 4.10: Comparison between various methods of evaluating the radius profiles for medium thickness shell ($C_2 = 10^6$), $C_3 = 0.4$, $C_4 = 10^2$ (average gas diffusivity) and initial gas pressure $P_{g0}^* = 15$.	58

CHAPTER 1

INTRODUCTION

Modeling the phenomenon of bubble growth in liquids is important to processes involving boiling, cavitation, bubble removal during glass making, micro-gravity studies, composite materials, manufacturing void-free high performance materials, measuring the elongation viscosity and polymer processing. The objective in foam processing is to manufacture lightweight articles with densities lower than the density of the polymer without significantly compromising the mechanical and physical properties of the products. Lower densities can be achieved by introducing a gas in the form of bubbles into the polymer. Gases may be introduced into a polymer by two different methods. In the first method, the polymeric pellets are compounded with an organic substance (blowing agent) in the pellet of powdered form. In the second method, an inert gas is dissolved in the polymer either in the solid stage (micro cellular foam) or in the molten stage under high pressures (foam injection molding). Pressure is then reduced carefully to allow the formation of bubbles in a controlled manner.

Three important phenomena govern the growth or collapse of bubbles in liquids, namely mass, momentum and energy transfer between the bubbles and the liquid. The transfer of mass can be either due to the phase change at the bubble interface or due to the diffusion of mass from the liquid into the bubble or both. In addition the rheological characteristics of the liquid surrounding the bubble will affect the growth process. The subject of this study is to improve on current models to investigate the bubble growth phenomenon in

highly viscous fluids. This work is particularly relevant to bubble growth associated with the processing of foams.

Boiling and cavitation studies motivated the early studies on bubble growth in liquids. In these studies, the growth of a single bubble was assumed to occur in a large body of liquid with the main mechanisms for the growth of the bubble being the momentum transfer between the bubble and the surrounding liquid, and the heat transfer-induced mass diffusion due to the phase change. Viscous effects in these cases were not important compared to the inertia and surface tension was ignored. There are practical cases where viscous effects during the bubble growth or collapse are important and cannot be ignored. Bubble growth or collapse during polymer processing and glass making are among such cases.

Polymer processing in general and foam processing in particular occur under non-isothermal conditions with heat transfer to the surrounding through the mold walls. The heat transfer has an impact on the properties of the gas-polymer system, some which, such as the melt viscosity, change by an order of magnitude during the non-isothermal process. The heat transfer does not change the qualitative features of the bubble growth process but it does effect the quantitative predictions.

Issues

Earlier studies to solve for the evolution of the bubble radius involved generally an infinite medium around the bubble and an infinite amount of gas is available for diffusion

into the bubble. Thus we obtain a bubble that is ever growing, but the reality is that in polymer foam processing there is no infinite shell of fluid surrounding the bubble and hence the amount of gas available for diffusion into the bubble is also limited. When a finite thickness shell of liquid surrounds the bubble, the size of the bubble reaches a maximum value and should stop growing unless there are other modes of increasing the bubble size.

Earlier models of bubble growth involved using polynomial profile approximations for the concentration of gas inside the liquid surrounding the bubble. The concentration of gas inside liquid surrounding the bubble was assumed to be invariant outside a concentration boundary layer of finite thickness. In this way the three coupled equations i.e. mass, momentum and diffusion equations were simplified to two coupled equations. The assumption of a polynomial concentration profile simplified the coupled equations and allowed for easily solving the coupled equations numerically. The polynomial profiles seem to match the complete solutions obtained by Arefmanesh et al., under certain conditions [1]. Interestingly the solutions matched at initial times, but the growth rate projected starts diverging after a certain point. This leads one to believe that the theory does not take into account the point when the concentration boundary layer hits the outer shell of the fluid. The solutions obtained seem to diverge when the concentration boundary layer hits the outer shell. The reason is that the boundary conditions change when the concentration boundary layer hits the outer shell. Moreover the theory also does not incorporate the finiteness of the shell into the solution.

Motivation

The main objective of this analysis is to develop an improved model for bubble growth in a liquid shell using the previously developed models based on approximate polynomial profiles. The usage of polynomial profiles not only results in simplicity and less numerical complexity, but they also give results in good agreement with the results obtained by Arefmanesh et al. [1]. Thus to take into account the case of bubble growth in a finite shell of liquid this study was taken up. Since the polynomial profiles give reasonable results during initial times, they were retained to develop a better solution for the bubble growth. Using polynomial profiles also decreases the numerical complexity in arriving at the solution.

CHAPTER 2

LITERATURE REVIEW

Literature on bubble growth can be divided into two main categories, studies on the bubble nucleation and the studies on the bubble growth. Nucleation of bubbles in single component systems, such as boiling of water, is relatively well understood in simple systems and can be described by the classical nucleation theory. On the contrary, nucleation of bubbles in multi-component systems, such as bubble nucleation during polymer processing, is not well understood. The existing theories of bubble nucleation in such systems are mainly modifications to the classical nucleation theory. On the other hand, there exists a rich body of literature on the growth or collapse of bubbles in liquids. The growth process of a bubble begins with the nucleation of a bubble.

Bubble Nucleation in Liquids

Nucleation is a physical phenomenon during which the initial fragments of a new and more stable phase are generated within a metastable phase, developing spontaneously into gross fragments of the stable phase. An example is boiling, which is due to nucleation and growth of vapor bubbles in superheated water. There are different mechanisms for bubble nucleation in liquids, namely, homogeneous, heterogeneous and mixed mode. In the homogeneous nucleation a vapor embryo of the critical radius can be formed by the normal statistical fluctuations of the liquid. In the heterogeneous mode, nucleation occurs at an interface between the volatile liquid and the other phase in contact. The mixed mode allows for both homogeneous and heterogeneous nucleation.

The nucleation phenomenon in polymer processing is far more difficult than the bubble nucleation in water, which can be described by classical nucleation theory. Due to lack of a reliable theory, the nucleation is generally assumed to be heterogeneous and instantaneous. It is often described with empirical relationships tailored to specific systems.

Bubble Growth in Inviscid liquids

Before addressing bubble growth in viscous liquids, early developments of bubble growth in inviscid liquids are briefly introduced to distinguish the phenomenon and the driving mechanisms from viscous liquids.

Early studies on bubble dynamics in liquids were motivated by problems such as boiling and cavitation in water. In these single component systems, the bubble growth is controlled by two distinct mechanisms, namely, the momentum transfer and the mass transfer due to evaporation and diffusion of heat. Under these conditions, the viscous term in the momentum equation is negligible compared to the inertia and the surface tension.

Rayleigh in his pioneering work investigated the bubble growth controlled by inertia forces [3]. Later, Plesset et al. [4,5], Froster et al. [6], Dergarabedian [7] and Birkhoff et al. [8], investigated the heat diffusion-induced growth of a spherical vapor bubble in a large body of superheated liquid and obtained analytical solution for asymptotic cases. Scriven investigated the spherically symmetric growth of a vapor bubble in an unlimited

body of superheated liquid when momentum transfer and diffusion of heat controlled the growth [9].

Rosner and Epstein investigated the effects of surface tension and the non-zero initial bubble size on the growth of a bubble controlled by both mass diffusion and momentum transfer [10]. They considered the cases in which the bubble growth rate departed from the parabolic growth rate predicted by Scriven. They assumed that the gas concentration gradient in the liquid was restricted to a small boundary layer close to the bubble interface and used the integral method to solve the diffusion equation. Their approach has been extensively used in solving diffusion-induced growth of gas bubbles in inviscid liquids.

In studying the bubble growth in liquids, there are cases where a number of gases diffuse into the bubble simultaneously. Cable et al. [11,12], and Ward et al. [13] investigated such cases.

The driving mechanisms for the bubble growth in inviscid liquids are the momentum transfer, the diffusion of mass due to evaporation, and the diffusion of dissolved gases present in the liquid. In inviscid fluids, the viscous effects are negligible as compared to the inertia, pressure and surface tension. On the contrary, the driving mechanisms for the bubble growth in viscous liquids are the momentum transfer and the gas diffusion. The viscous effects, in this case, are dominant and the inertia terms in the momentum equation are negligible due to the low Reynolds numbers.

Bubble Growth in Viscous liquids

In the bubble phenomenon, during polymer processing in general and foam molding in particular, the simultaneous mass, momentum and energy transfer between the bubble and the polymer are important. There are also other issues in foam processing, such as concentration of the dissolved gas in the polymeric melt, the pressure distribution in the mold and the diffusivity of the gas in the polymer, which have significant effects on the bubble growth. Barlow et al. [14], Longlois [15], Szekely et al. [16], Yung et al. [17] and Patel [18] studied the diffusion-induced growth of a spherical gas bubble in a large body of Newtonian liquid containing a dissolved gas under isothermal conditions. Szekely et al. and Patel obtained numerical solutions by assuming polynomial profiles for the concentration of dissolved gas in the fluid around the bubble while Barlow et al. obtained analytical solutions for the asymptotic stages of the growth by assuming that the gas concentration was limited to a thin boundary layer close to the bubble interface (thin shell approximation) outside of which the concentration remained equal to the initial concentration. This enabled them to eliminate the convective term in the diffusion equation. Their results showed that initially the growth was a linear function of time.

However, in the final asymptotic stage it followed the well-known parabolic behavior. Qiu et al. investigated the dynamics of a single bubble during pool boiling and under low gravity conditions [19]. They obtained experimental results on the growth and detachment mechanisms of a single bubble on a heated surface conducted during the parabolic flights of aircrafts.

Prodanovic et al. investigated the bubble behavior in sub-cooled flow boiling of water at low pressures and low flow [20]. Prodanovic et al. obtained experimental data by varying the pressure, bulk liquid velocities and sub-cooling temperature.

Robinson and Judd investigated the bubble growth in a uniform and spatially distributed temperature field [21]. A theory was developed which was shown to predict experimental bubble growth data for both spherical growth in an unbounded liquid and hemispherical growth at a heated plane surface in micro-gravity.

Miyatake et al. obtained a simple universal equation for vapor bubble growth in uniformly superheated pure liquids and in binary solutions with a non-volatile solute [22]. There are three regimes of growth process of the bubble: nucleation of the bubble, inertia controlled growth and heat transfer controlled growth. Once again this theory is limited by use in the case of infinite shell of liquid surrounding the bubble. Moreover Miyatake et al. did not consider growth process through diffusion.

Venerus et al. developed transport models for diffusion induced bubble growth in viscoelastic liquids and evaluated those models [23]. They took into consideration the convective and diffusive mass transport as well as surface tension and inertial effects. Venerus et al. developed a rigorous model for the transport analysis of diffusion induced bubble growth and collapse in viscous liquids [24]. They showed that other models could be derived from their model using different mathematical models and dimensional

analysis. This model is limited by its applicability in the case of a bubble surrounded by an infinite amount of liquid only.

Venerus also developed models for bubble growth in viscous liquids of finite and infinite extent [25]. These models are similar to that obtained Arefmanesh et al. Both these methods for evaluating the bubble growth are difficult to solve numerically due to coupled equations.

Summary

To summarize the contribution of relevant literature to the subject of investigation in this thesis, as the nucleation of the bubbles in polymeric liquids is concerned, at present there does not exist a reliable theory, which can predict the bubble nucleation accurately. On the other hand, the bubble growth phenomenon has been extensively studied both in inviscid and viscous liquids with emphasis on different aspects of the phenomenon. There have also been experimental as well as numerical studies on the bubble growth during polymer processing covering issues such as mass transfer, momentum transfer and solubility and diffusivity of the dissolved gases in the polymer. These studies are either restricted to the growth of a bubble in large body of polymer melt or in the case of foam molding, where bubbles are separated by thin films of the polymeric melt, they are confined to the growth of an average bubble as a representative of all the bubbles in the mold.

The use of polynomial profiles to solve for the growth rate of the bubble simplifies the equations and also the numerical complexity. But their usage has been limited to the case of infinite medium of liquid surrounding the bubble. This restricts the practical usability of the model. Therefore the polynomial profiles have been used in this thesis work to solve for bubble growth rates for a finite shell of liquid surrounding the bubble. The reasons for the disharmony in the results obtained by polynomial profile solutions and those obtained by Arefmanesh et al. are also investigated.

CHAPTER 3

THEORY OF SINGLE BUBBLE GROWTH

This chapter contains a review of theory of a single bubble growth in viscous Newtonian liquids. The bubble is assumed to be surrounded by an infinite amount of liquid. The equations governing the growth of a single bubble in a large body of liquid are stated. Their modifications to bubble growth in a liquid shell with finite thickness and a limited amount of dissolved gas are presented in the next chapter.

Growth of a Bubble in an Infinite Newtonian Medium

Governing equations for bubble growth in highly viscous liquids such as polymer melts are derived. The Reynolds number for these liquids is much smaller than one. Therefore, the inertia terms in the momentum equation are neglected. It is assumed that the concentration of the dissolved gas at the bubble interface is related to the gas pressure inside the bubble through the Henry's law. Henry's law is a special case of the Raoult's law and is valid for low concentrations [27]. This study focuses on liquids with low gas concentration. It is also assumed that the gas inside the bubble behaves as an ideal gas. The bubble growth considered in this chapter is due to both mass and momentum transfer which are coupled through the movement of the bubble interface. In the following sections, the equations governing these phenomena in Newtonian liquids are presented. In order to simplify the analysis the whole process is assumed to occur under isothermal conditions.

Hydrodynamics of the growth process

It is assumed that nucleation has occurred and a bubble with radius R_0 that is greater than the critical radius necessary for growth has been produced. Consider the growth of this spherical bubble in an unlimited body of viscous Newtonian liquid. To study the spherically symmetric growth of the bubble, a spherical coordinate system with its origin at the center of the bubble is chosen. Figure (3.1) shows a schematic of the bubble in a large body of liquid. The expansion of the bubble generates an extensional flow field in the liquid surrounding the bubble. The equation of continuity for the liquid in the spherical coordinate system is given by

$$\frac{\partial \rho}{\partial t} + \frac{1}{r^2} \frac{\partial}{\partial r} (\rho r^2 v_r) + \frac{1}{r \sin \theta} \frac{\partial}{\partial \theta} (\rho v_\theta \sin \theta) + \frac{1}{r \sin \theta} \frac{\partial}{\partial \phi} (\rho v_\phi) = 0 \quad (3.1)$$

where ρ is the density of the liquid and v_r , v_θ , and v_ϕ are the components of the velocity. The assumption of spherical symmetry allows one to simplify the problem. The flow field around the bubble is purely extensional and the only non-zero component of the velocity is the non-radial component (v_r). Hence the continuity equation reduces to the following

$$\frac{\partial \rho}{\partial t} + \frac{1}{r^2} \frac{\partial}{\partial r} (\rho R^2 v_r) = 0 \quad (3.2)$$

The boundary condition for the above equation is given by

$$v_r = \dot{R} \quad (3.3)$$

where \dot{R} is the rate of change of the bubble radius with respect to time.

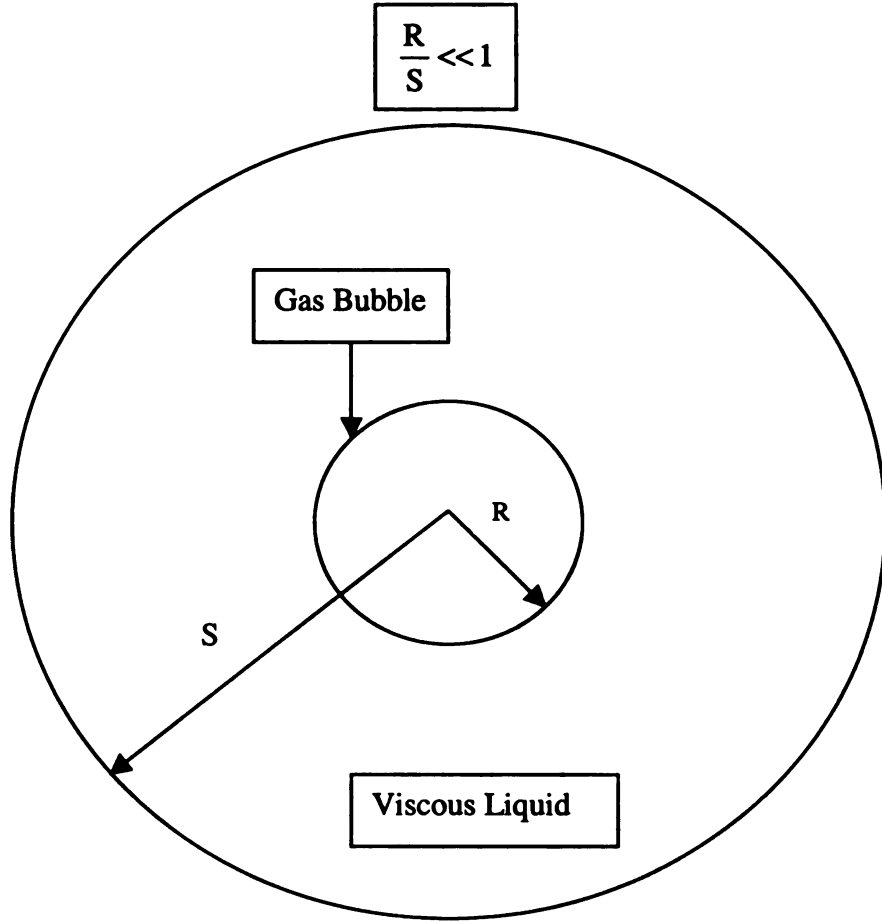


Figure 3.1: Schematic of a spherical bubble growing in an infinite medium

Since the density of the liquid is only a function of temperature, equation (3.2) can be easily integrated to yield the velocity field. Integrating equation (3.2) and using the boundary condition at the interface (equation (3.3)) results in the following velocity field:

$$v_r = \frac{R^3 - r^3}{3r^2} \frac{\dot{\rho}}{\rho} + \frac{R^2}{r^2} \dot{R} \quad (3.4)$$

where $\dot{\rho}$ is the derivative of the liquid density with respect to time. Under isothermal conditions, the density of the liquid does not change with respect to time and hence the first term on the right hand side of equation (3.4) can be neglected. After simplification the velocity field reduces to the following well-known equation

$$v_r = \frac{R^2 \dot{R}}{r^2} \quad (3.5)$$

The conservation of momentum for the liquid around the bubble in the radial direction in terms of stresses is given by

$$\rho \left(\frac{\partial v_r}{\partial t} + v_r \frac{\partial v_r}{\partial r} \right) = -\frac{\partial P}{\partial r} + \frac{1}{r^2} \frac{\partial}{\partial r} \left(r^2 \tau_{rr} \right) - \frac{\tau_{\theta\theta} + \tau_{\phi\phi}}{r} \quad (3.6)$$

where P is the liquid pressure, and τ_{rr} , $\tau_{\theta\theta}$ and $\tau_{\phi\phi}$ represent the stresses in the liquid.

$\tau_{\theta\theta}$ is equal to $\tau_{\phi\phi}$ due to spherical symmetry. For a Newtonian liquid and the velocity field given by equation (3.5), the stresses are readily evaluated in terms of the bubble radius. Using the results in equation (3.6) reduces the momentum equation to the following

$$\frac{\partial P}{\partial r} - \frac{\partial \tau_{rr}}{\partial r} - 2 \frac{\tau_{rr} - \tau_{\theta\theta}}{r} = \rho \left(2 \frac{\dot{R}^2 R^4}{r^5} - 2 \frac{\dot{R}^2 R}{r^2} - \frac{\ddot{R} R^2}{r^2} \right) \quad (3.7)$$

where ρ is the density of the liquid and \ddot{R} is the second derivative of the bubble radius with respect to time. To relate the gas pressure inside the bubble to the bubble radius and the applied pressure in the liquid, equation (3.7) is integrated with respect to the radial coordinate from the bubble interface R to infinity [12].

The integrated momentum equation is given by

$$\rho \left(\frac{3}{2} \ddot{R}^2 + \dot{R} \ddot{R} \right) = p(R) - P(\infty) + \tau_{rr}(R) - \tau_{rr}(\infty) + 4 \frac{\eta \dot{R}}{R} \quad (3.8)$$

$P(R)$ and $P(\infty)$ are the liquid pressures at the bubble interface and infinity respectively.

η is the liquid viscosity. The following relation gives the condition of stress continuity at the bubble-liquid interface:

$$-P_g + \frac{2\sigma}{R} = -P(R) + \tau_{rr}(R) \quad (3.9)$$

where P_g is the gas pressure inside the bubble and σ is the surface tension. Substituting the expression for the liquid pressure at the interface ($P(R)$) from equation (3.9) into equation (3.8) yields the following equation for the momentum transfer in a large body of Newtonian liquid

$$\rho \left(\frac{3}{2} \ddot{R}^2 + \dot{R} \ddot{R} \right) + 4\eta \frac{\dot{R}}{R} + \frac{2\sigma}{R} + P_\infty - P_g = 0 \quad (3.10)$$

where P_∞ is the applied pressure at infinity. The momentum equation relates the gas pressure inside the bubble to the bubble radius and the applied pressure. The first three terms in this equation represent the inertia, viscous and surface tension effects. In general, for highly viscous liquids such as polymer melts the inertia terms are negligible and the viscous forces play a significant role. In this study the inertia terms are neglected.

Mass diffusion

To determine the gas pressure inside the bubble, the principle of conservation of mass is applied to the gas inside the bubble, which results in the following ordinary differential equation [12]

$$\frac{d}{dt}(\rho_g R^3) = 3\rho_g D R^2 \left(\frac{\partial C_A}{\partial r} \right)_{r=R} \quad (3.11)$$

where ρ_g is the density of the gas inside the bubble, D is the diffusion coefficient of the dissolved gas in the liquid, and $\left(\frac{\partial C_A}{\partial r} \right)_{r=R}$ is the concentration gradient of the dissolved gas at the bubble interface. The left hand side of equation (3.11) is the rate of accumulation of mass inside the bubble and the right hand side is the rate of diffusion of gas from the liquid into the bubble.

At this point two assumptions pertaining to the gas inside the bubble are made. First, it is assumed that the gas inside the bubble behaves as an ideal gas. Considering that the gas pressure inside the bubble is relatively low, the ideal gas assumption is reasonable [28]. Second, it is assumed that the concentration of the dissolved gas at the bubble interface is related to the gas pressure inside the bubble through Henry's law [12]

$$C_A(R, t) = C_W(t) = K_h P_g(t) \quad (3.12)$$

where C_W is the concentration of the dissolved gas at the bubble interface and K_h is the Henry's constant. Henry's law is in general valid for glassy polymers at elevated temperatures. It is assumed that the dissolved gas is initially uniformly distributed in the

liquid around the bubble with concentration C_0 . This corresponds to an initial gas pressure of P_{g0} , which is related to the initial gas concentration through the Henry's law.

However, the pressure inside the bubble decreases as the bubble expands in accordance with the ideal gas law. Consequently, the concentration of the dissolved gas at the interface also decreases in accordance with Henry's law. This will create a concentration gradient in the liquid around the bubble and invokes the diffusion of the dissolved gas into the bubble. The diffusion of the dissolved gas from the liquid into the bubble is governed by the Fick's law of diffusion in the spherical coordinate system

$$\frac{\partial C_A}{\partial t} + v_r \frac{\partial C_A}{\partial r} = D \left[\frac{1}{r^2} \frac{\partial}{\partial r} \left(r^2 \frac{\partial C_A}{\partial r} \right) \right] \quad (3.13)$$

where D is the diffusivity of the gas in the polymer melt, and C_A is the weight fraction of the gas dissolved in the melt.

To solve equation (3.11) for the gas pressure inside the bubble, one needs to know the concentration gradient at the interface. Therefore it is necessary to solve equation (3.13) to obtain the concentration profile first. There are different approaches for solving the diffusion equation. Either it may be written in difference form and solved in its entirety or approximate solutions may be sought. The approximate solutions have certain advantages over the more difficult to solve complete equation set. One of the advantages is its simplicity and their reasonable accuracy in the results obtained.

Integral method

The integral method is the most widely used approximate method in phase change problems. This approximate method of solving partial differential equations dates back to von Karman and Pohlhausen who used the method to solve the boundary layer equations [29]. There are four basic steps in applying the integral method to the diffusion equation [30]. First the diffusion equation is integrated over a phenomenological distance $\delta(t)$ called the diffusion boundary layer. Second a polynomial profile is chosen for the concentration distribution in the boundary layer. The coefficients of the polynomial are evaluated in terms of the boundary layer thickness by utilizing the boundary conditions. Third the polynomial profile is introduced in the integral equation and an ordinary differential equation (ODE) for $\delta(t)$ is obtained. Finally the solution of the ODE yields the concentration profile in the liquid.

In employing the integral method, it is assumed that the concentration gradients are limited to a small boundary layer close to the bubble interface, outside of which the gas concentration remains virtually undisturbed and equal to the initial concentration [6]. This assumption may be reasonable under special circumstances such as bubble growth in a large body of liquid and early stages of growth. However, it is not in general valid and may overestimate the final bubble radius. To obtain approximate solutions, second order and third order profiles are assumed in this study.

The momentum and diffusion equations are coupled and as the bubble grows, the bubble gas pressure P_g will decrease, giving rise to a concentration gradient at the bubble wall,

which in turn affects the mass transfer process. The concentration on the wall of the bubble $C_W(t)$ can be described by the Henry's Law

$$C_A(R, t) = C_W(t) = K_h P_g(t) \quad (3.14)$$

Assuming that the gas follows the ideal gas law,

$$P_g(t) = \frac{R_g T \rho_g(t)}{M} \quad (3.15)$$

where M and ρ_g are the molecular mass and density of the gas respectively. Combining equations (3.14) and (3.15) we have

$$\rho_g(t) = \frac{C_W(t)M}{R_g T K_h} \quad (3.16)$$

The conservation of mass at the bubble interface is from equation (3.11)

$$\frac{d}{dt}(\rho_g R^3) = 3\rho_g R^2 \left(\frac{\partial C_A}{\partial r} \right)_{r=R} \quad (3.17)$$

In order to solve the equations (3.10, 3.13 and 3.17) simultaneously the integral method is adopted. In this method, the diffusion equation is multiplied with r^2 and integrated from with respect to r from $r = R$ to $r = R + \delta$, in which δ is the concentration boundary layer. After integrating and using the following relationships:

$$r^2 v_r = R^2 \dot{R} \quad (3.18)$$

$$C_A(R + \delta) = C_0, C_A(R) = C_W \text{ and } \frac{\partial C_A}{\partial r} = 0 \text{ at } r = R + \delta \quad (3.19)$$

where \dot{R} is the radius R differentiated with respect to time, which is the velocity of the bubble surface. We then obtain

$$\frac{d}{dt} \int_R^{R+\delta} (C_A - C_0) r^2 dr = -DR^2 \left(\frac{\partial C_A}{\partial r} \right)_{r=R} \quad (3.20)$$

Using the mass flux equation (equation (3.11)) we obtain

$$3\rho \int_R^{R+\delta} \left(\frac{C_0 - C_A}{C_0 - C_W} \right) r^2 dr = \frac{\rho_g R^3 - \rho_{g0} R_0^3}{C_0 - C_W} \quad (3.21)$$

where ρ_{g0} is the density of the gas bubble at $t = 0$, and R_0 is the initial bubble radius.

Now the concentration profile is assumed to be a polynomial. If a second-degree polynomial is assumed then we have:

$$\frac{C_0 - C_A}{C_0 - C_W} = \left(1 - \left(\frac{r - R}{\delta} \right) \right)^2 \text{ for } R < r < R + \delta \quad (3.22)$$

$$\frac{C_0 - C_A}{C_0 - C_W} = 0 \text{ for } r > R + \delta \quad (3.23)$$

and substitution of equations (3.22) and (3.23) in the left hand side of equation (3.21) results in

$$3\rho \left[\frac{1}{30} \left(\frac{\delta}{R} \right)^3 + \frac{1}{6} \left(\frac{\delta}{R} \right)^2 + \frac{1}{3} \left(\frac{\delta}{R} \right) \right] R^3 = \frac{\rho_g R^3 - \rho_{g0} R_0^3}{C_0 - C_W} \quad (3.24)$$

Neglecting the terms containing $(\delta/R)^2$ and higher order terms we have

$$\delta = \frac{\rho_g R^3 - \rho_{g0} R_0^3}{\rho(C_0 - C_W) R^2} \quad (3.25)$$

Substituting equation (3.25) into the right hand side of equation (3.18) and eliminating δ from the resulting expression we obtain

$$\frac{d}{dt}(\rho_g R^3) = \frac{6\rho^2 D(C_0 - C_w)R^4}{\rho_g R^3 - \rho_{g0}R_0^3} \quad (3.26)$$

If $(\delta/R)^2$ and lower order terms are also considered we get

$$\delta = -R + \sqrt{R^2 + \frac{2B}{R}} \quad (3.27)$$

$$B = \frac{\rho_g R^3 - \rho_{g0}R_0^3}{\rho(C_0 - C_w)} \quad (3.28)$$

we obtain

$$\frac{d}{dt}(\rho_g R^3) = \frac{6\rho D(C_0 - C_w)R^2}{(R^2 + \frac{2B}{R})^{(\frac{1}{2})} - R} \quad (3.29)$$

If a third order profile is used for the concentration in the liquid and neglecting the higher order terms i.e. $(\delta/R)^2$ and higher, we get

$$\frac{d}{dt}(\rho_g R^3) = \frac{27\rho^2 D(C_0 - C_w)R^4}{4(\rho_g R^3 - \rho_{g0}R_0^3)} \quad (3.30)$$

To obtain the second order profile, the gas concentration was assumed to be equal to the initial gas concentration and gradient of the concentration was assumed to be zero outside the boundary layer. To obtain equation (3.30), second derivative of the gas concentration was also assumed to be zero outside the boundary layer.

Equation (3.10) together with equation (3.26) or equation (3.30) constitute the governing equations for the growth of a bubble in a large body of Newtonian liquid with the assumption of a second order or a third order profile for the gas concentration. The

unknowns in these equations are the bubble radius and the gas pressure or the gas density inside the bubble. The initial conditions for these equations are

$$R(t = 0) = R_0 \quad (3.31)$$

$$P_g(t = 0) = P_{g0}$$

The solution to these equations yields the bubble radius and the gas pressure inside the bubble as a function of time. In order to solve the equations and provide the results in a more effective manner the equations are made dimensionless and solved for the dimensionless parameters.

The momentum equation (equation (3.10)) along with equations (3.26) or (3.30) are made dimensionless using the following parameters

$$P_g^* = \frac{P_g}{P_a} \quad (3.32)$$

$$P_f^* = \frac{P_f}{P_a} \quad (3.33)$$

$$R^* = \frac{R}{R_0} \quad (3.34)$$

$$t^* = \frac{t}{t_{ref}} \quad (3.35)$$

$$\xi^* = \frac{P_g R^3 - P_{g0} R_0^3}{P_{g0} R_0^3} \quad (3.36)$$

Dimensional analysis shows that t_{ref} , which is related to the momentum transfer, is equal to η/P_a . The momentum equation after inserting the dimensionless parameters is given by

$$4 \frac{dR^*}{dt^*} = \frac{(1 + \xi^*) P_{g0}^*}{R^{*2}} - P_f^* - C_3 \quad (3.37)$$

Equation (3.26) is converted to dimensionless form using the parameters in equations (3.32), (3.33), (3.34), (3.35) and (3.36). We get

$$\frac{d\xi^*}{dt^*} = \frac{C_4 C_7}{\xi^*} (R^{*3} - \xi^* - 1)^2 \frac{1}{R^{*2}} \quad (3.38)$$

Equation (3.38) is singular at $t^* = 0$, therefore the following transformation is used.

$$\zeta^* = \xi^{*2}, \quad \zeta^*(0) = 0 \quad (3.39)$$

Substituting equation (3.39) in equation (3.38) the reduced mass-balance equation becomes

$$\frac{d\zeta^*}{dt^*} = 2C_4 C_7 \frac{(R^{*3} - \sqrt{\zeta^*} - 1)^2}{R^{*2}} \quad (3.40)$$

where the constants C_3 , C_4 and C_7 are given in Table (3.1). C_7 depends on the type of polynomial profile approximation being used. The expressions for C_7 , for second and third order polynomial profiles are also shown in Table (3.1). The physical significance of these constants will be explained in chapter 4. The boundary conditions for these sets of equations are

$$R^*(0) = 1 \quad (3.41)$$

$$\zeta^*(0) = 0 \quad (3.42)$$

Summary

In this chapter the governing equations for the growth of a single bubble in viscous Newtonian liquids were reviewed. The Integral method was used to modify the diffusion equation. The integrated diffusion equation was also modified using the interfacial mass balance. Then second and third order polynomial concentration profiles were substituted into the modified diffusion equation (equation (3.21)). The resulting diffusion equation was then solved along with the momentum equation using the boundary conditions. The results are then plotted and compared to various other methods of obtaining bubble growth profiles. The plots are shown in the next chapter.

Table 3.1: Expressions for the constants C_2 , C_3 , C_4 , C_5 , C_6 and C_7

C_2	$\frac{S_0^3}{R_0^3} - 1$
C_3	$\frac{2\sigma}{R_0 P_a}$
C_4	$\frac{D\mu}{R_0^2 P_a}$
C_5	$\frac{\rho R_g T}{P_a}$
C_6	$K_h P_a$
C_7	$6\rho^2 k_h^2 (R_g T)^2$ Second order polynomial profile $\frac{27\rho^2 k_h^2 (R_g T)^2}{4}$ Third order polynomial profile

CHAPTER 4

GROWTH OF A GAS BUBBLE IN A LIMITED BODY OF NEWTONIAN LIQUID

In this chapter, the equations governing the growth of a gas bubble in a limited body of Newtonian liquid are presented. This is representative of a situation when a large number of bubbles are separated by small distances grow in the liquid. In the earlier approach, using a polynomial profile, the gas concentration far from the bubble was assumed to be equal to the initial concentration at all times. Hence although the diffusion process slows down and its rate reduces with time, it will never be zero. This will result in over-prediction of the final bubble radius. Therefore it is necessary to solve the equation in a different manner by taking into account the finite thickness of the liquid shell surrounding the bubble. The assumptions of Henry's law at the gas-bubble interface are still valid though.

Three different techniques of predicting the bubble growth behavior in a finite thickness shell are developed. These results are then compared with the bubble growth behavior in an infinite medium predicted using approximate polynomial profiles for the gas concentration and the results obtained by Arefmanesh [1]. Arefmanesh obtained the bubble growth behavior by solving the full diffusion equation. Then the regimes under which the assumption of polynomial profile breaks down are investigated by comparing the approximate solutions with the solutions obtained by solving the full diffusion equation.

Hydrodynamics of the growth in a shell of Newtonian liquid

To analyze the growth of a gas bubble in a finite body of liquid, a spherical gas bubble surrounded concentrically by a liquid shell with finite thickness and constant mass is considered. This configuration, which ensures spherical symmetry, is shown in fig (4.1). In this figure, $R(t)$ is the radius of the bubble and $S(t)$ is the radius of the outer shell. It is assumed that the bubble growth occurs under isothermal conditions. Therefore, the volume of the liquid shell remains constant throughout the process. The kinematics of the flow in this case remains the same as before and the velocity field is given by the equation (3.5). The momentum equation is given by eq (3.7). However in this case the momentum equation is integrated between the bubble interface (R) and the outer radius of the shell (S). The integrated momentum equation is given by

$$\rho \left(\frac{1}{2} \dot{R}^2 R^4 \left(\frac{1}{S^4} - \frac{1}{R^4} \right) - \left(\ddot{R} R^2 + 2 \dot{R}^2 R \right) \left(\frac{1}{S} - \frac{1}{R} \right) \right) = \quad (4.1)$$

$$- P(S) + P(R) + \tau_{rr}(S) - \tau_{rr}(R) + 4\eta \dot{R} R^2 \left(\frac{1}{S^3} - \frac{1}{R^3} \right)$$

The condition of stress continuity (equation (3.9)) at the bubble interface is applied again here. Equation (4.1) can then be written as

$$\rho \left(\frac{1}{2} \left(\psi^{\frac{4}{3}} - 1 \right) R \dot{R}^2 - \left(\psi^{\frac{4}{3}} - 1 \right) \left(R^2 \ddot{R} + 2 R \dot{R}^2 \right) \right) = \quad (4.2)$$

$$(P_g - P_f) R - 2\sigma + 4\eta(\psi - 1) \dot{R}$$

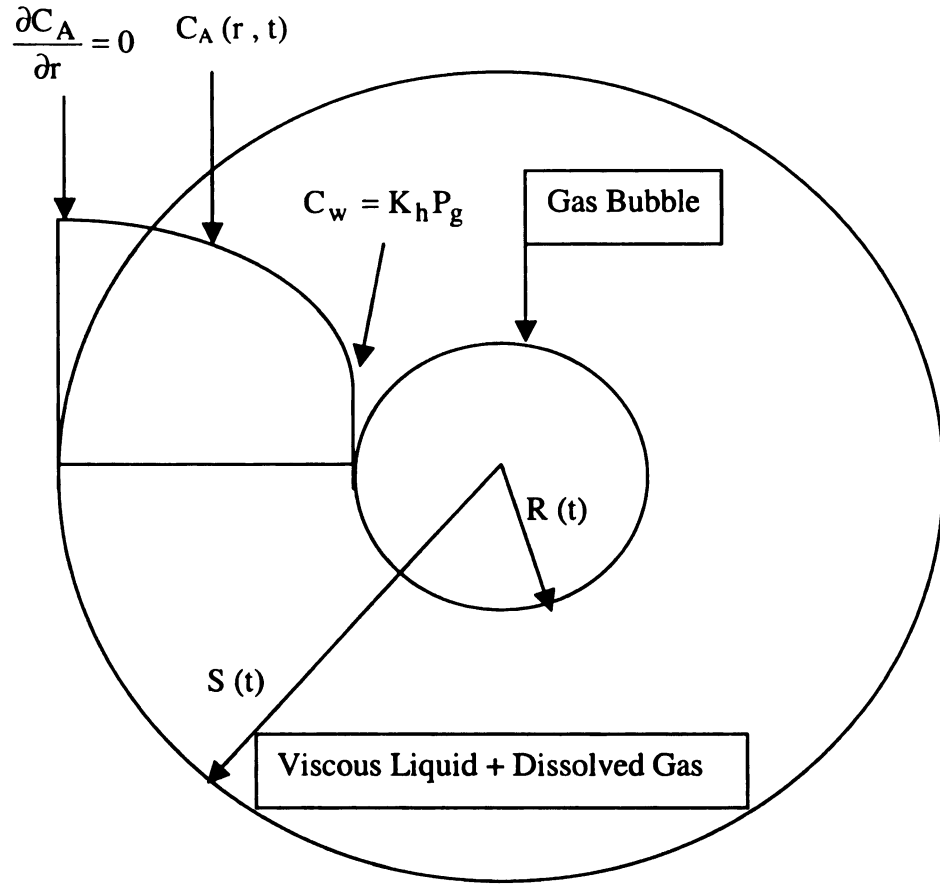


Figure 4.1: Schematic of a bubble in a shell of viscous liquid containing dissolved gas

Where $\psi = \frac{R^3}{V + R^3}$, V is equal to $S^3 - R^3$ and is proportional to the volume of the liquid surrounding the bubble and P_f is the applied pressure at the outer boundary of the liquid shell. For a high viscosity liquid i.e. when the viscous forces are dominant over inertia forces then the left hand side of the above equation can be neglected as shown in chapter 3.

$$(P_g - P_f)R - 2\sigma + 4\eta(\psi - 1)\dot{R} = 0 \quad (4.3)$$

Converting it to dimensionless form

$$\frac{4(C_2 + 1 - R^{*3})}{1 + C_2} R^* = \frac{(1 + \xi^*) P_{g0}^*}{R^{*2}} - P_f^* R^* - C_3 \quad (4.4)$$

Equation (4.4) governs the momentum transfer between the bubble and the liquid shell. If the volume of the liquid in the shell is much greater than the bubble volume, this equation reduces to the momentum equation (equation (3.37)) derived previously.

Diffusion of mass in the liquid shell

The conservation of mass for the dissolved gas in the liquid shell is described by the equation (3.11). The diffusion of gas from the liquid shell into the bubble is governed by the equation (3.13). However in this case the radial distance is confined between the bubble radius and the outer radius of the spherical shell. The main difference between the current and the previous case is that the amount of liquid surrounding the bubble is limited now. Therefore, the amount of gas will also be limited now. This issue is directly related to the boundary condition for the diffusion equation at the outer radius of the liquid shell. The correct boundary condition, which expresses the physics of the problem, is that the gradient of the gas concentration at the outer boundary of the liquid should be equal to zero. Earlier it was assumed the concentration outside the boundary layer is always equal to the initial concentration. Hence the gas concentration at the outer boundary always equals the initial concentration. This implies that all the derivatives of the concentration are equal to zero outside the boundary layer and at the outer boundary of the shell. However for a bubble surrounded by a limited body of liquid, the concentration at the outer boundary of the liquid is not equal to the initial concentration

but decreases as more and more gas diffuses into the bubble. However as the liquid in the shell around the bubble does not exchange mass with the surroundings, all derivatives of the concentration are equal to zero at the outer boundary of the liquid. This is also the case at the line of symmetry between the two bubbles.

The diffusion equation in spherical coordinate system

$$\frac{\partial C_A}{\partial t} + V_r \frac{\partial C_A}{\partial r} = D \left[\frac{1}{r^2} \frac{\partial}{\partial r} \left(r^2 \frac{\partial C_A}{\partial r} \right) \right] \quad (4.5)$$

In order to solve the set of equations the Integral Method adopted for infinite medium, will be used. The diffusion equation is multiplied with r^2 and integrated from with respect to r from $r = R$ to $r = S$, where S is the outer radius of the shell. After integrating and using the following relationships

$$r^2 v_r = R^2 \dot{R} \quad (4.6)$$

$$C_A(S) = C_S, \quad C_A(R) = C_W, \quad \text{and} \quad \frac{\partial C_A}{\partial r} = 0 \quad \text{at} \quad r = S \quad (4.7)$$

Where the first condition is obtained from the continuity equation as shown earlier in chapter 3. The second and third conditions mean that C_S and C_W give the concentration of the gas at the outer shell and the bubble-liquid interface respectively. The fourth condition means that the radial concentration gradient is zero at the outer end of the liquid shell.

We get

$$\frac{d}{dt} \int_R^S (C_A - C_S) r^2 dr + \int_R^S r^2 \frac{\partial C_S}{\partial t} dr = -D R^2 \left(\frac{\partial C_A}{\partial r} \right)_{r=R} \quad (4.7)$$

$$\frac{\partial C_S}{\partial t} = \frac{dC_S}{dt} \quad (4.8)$$

Equation (4.8) means that C_S is a function of time only. At this juncture the equation (4.7) needs to be looked into to make any good simplifications so that it can be evaluated easily.

There are different approaches that can be adopted at this juncture:

Using momentum equation along with

- 1) Diffusion equation and interfacial mass balance
- 2) Diffusion equation, interfacial mass balance and overall mass balance
- 3) Interfacial mass balance and overall mass balance

The various strategies to solve the equations are also shown in Table (4.1). Interfacial mass balance needs to be used because it simplifies the Right Hand Side of the integrated diffusion equation (4.7). Simplifying assumptions need to be made in order to solve the equations. The first approach makes simplifying assumptions in the second term in equation (4.7). The second method uses all the three governing equations to make simplifications. In the third method, the Fick's Law of diffusion equation is not used explicitly.

First approach

In this method of evaluation of the profile the following assumption is made

$$\frac{S^3 - R^3}{3} = \text{Constant} \quad (4.9)$$

This is a good assumption if the bubble radius of the same order of magnitude as the outer radius of the liquid shell. This will be a good assumption after the bubble has grown

to a certain size. There is another assumption that is similar to the one stated above and is similar in analogy. It can be assumed that the velocity of the liquid in the shell can be assumed to be negligible as the liquid is highly viscous. It will be shown that both these assumptions are not very much different from each other.

Table 4.1: Methods adopted to predict bubble growth behavior in finite shell bubble growth

	Momentum equation along with
Method 1	Diffusion equation and Interfacial mass balance equation
Method 2	Diffusion equation, Interfacial mass balance equation and Overall mass balance equation
Method 3:	Interfacial mass balance equation and Overall mass balance equation

Integrating equation (4.7) with respect to time from $t = 0$ to $t = t$ and utilizing the boundary equations, we get

$$\int_R^S \left(\frac{C_A - C_S}{C_W - C_S} \right) r^2 dr - \frac{C_S - C_0}{C_S - C_W} \left(\frac{S^3 - R^3}{3} \right) = \frac{1}{3\rho} \frac{\rho_g R^3 - \rho_{g0} R_0^3}{C_S - C_W} \quad (4.10)$$

Han and Yoo [26] derived equation (4.11) for gas bubble growing in an infinite medium as shown in chapter 3.

$$3\rho \int_R^{R+\delta} \left(\frac{C_0 - C_A}{C_0 - C_W} \right) r^2 dr = \frac{\rho_g R^3 - \rho_{g0} R_0^3}{C_0 - C_W} \quad (4.11)$$

A second order polynomial profile is assumed for the concentration profile and the boundary conditions substituted in it. This results in the following expression

$$\frac{C_A - C_S}{C_W - C_S} = \left(\frac{S - r}{S - R} \right)^2 \quad (4.12)$$

Substituting equation (4.12) in the first term on the left side of equation (4.10) and simplifying we get

$$M = \frac{3\rho}{(S - R)^2} \left(\frac{S^5}{30} - \frac{S^2 R^3}{3} + \frac{S R^4}{2} - \frac{R^5}{5} \right) \quad (4.13)$$

Substituting equation (4.13) in the diffusion equation (equation (4.10)) we get

$$C_S = \frac{\rho_g R^3 - \rho_{g0} R_0^3 + M C_W - \rho C_0 (S^3 - R^3)}{M - \rho (S^3 - R^3)} \quad (4.14)$$

The interfacial mass balance equation after substitution of expression of a second order polynomial concentration profile becomes

$$\frac{d}{dt} (\rho_g R^3) = \frac{6\rho D R^2}{(S - R)} (C_S - C_W) \quad (4.15)$$

Converting the expression for M into dimensionless form using the dimensionless parameters shown in Table (3.1) we have

$$M = \frac{3\rho R_0^3}{(S^* - R^*)^2} \left(\frac{S^{*5}}{30} - \frac{S^{*2} R^{*3}}{3} + \frac{S^* R^{*4}}{2} - \frac{R^{*5}}{5} \right) \quad (4.16)$$

using

$$\xi^* = \frac{P_g R^3 - P_{g0} R_0^3}{P_{g0} R_0^3} \quad (4.17)$$

C_S in dimensionless form can be written as

$$C_S = \frac{MK_h P_a P_g^* - \rho K_h P_a P_{g0}^* R_0^3 (S^{*3} - R^{*3}) + \frac{P_a R_0^3 P_{g0}^* \xi^*}{R_g T}}{M - \rho R_0^3 (S^{*3} - R^{*3})} \quad (4.18)$$

Substituting parameters from Table (3.1) into the mass balance equation (equation (4.15))

we get

$$\frac{d\xi^*}{dt^*} = \frac{6R_g T \mu \rho D}{R_0^2 P_a^2 P_{g0}^*} \left(\frac{R^{*2}}{S^* - R^*} \right) (C_S - C_W) \quad (4.19)$$

Using the transformation $\zeta^* = \xi^{*2}$ we get

$$\frac{d\zeta^*}{dt^*} = 2\sqrt{\zeta^*} (6C_4 C_5) \left(\frac{R^{*2}}{S^* - R^*} \right) \left(\frac{\frac{P_a R_0^3 \xi^*}{R_g T (M - \rho R_0^3 (S^{*3} - R^{*3}))} + \frac{MK_h P_a (1 + \xi^*)}{R^{*3} (M - \rho R_0^3 (S^{*3} - R^{*3}))} - \frac{\rho K_h P_a R_0^3 (S^{*3} - R^{*3})}{(M - \rho R_0^3 (S^{*3} - R^{*3}))} - \frac{C_6 (1 + \xi^*)}{R^{*3}}}{R^{*3}} \right) \quad (4.20)$$

The constants C_2 , C_3 , C_4 , C_5 and C_6 have a physical significance attached to them.

C_2 expresses the ratio of volume of the liquid to the initial bubble volume. C_3 is the dimensionless surface tension. C_4 represents the ratio of the time scale for the momentum transfer to the time scale of the gas diffusion. C_5 is the ratio of liquid to the gas density when the latter is evaluated at atmospheric pressure and C_6 is a dimensionless Henry's constant.

If a third order polynomial profile is used instead of second order profile we have

$$\frac{C_A - C_S}{C_W - C_S} = \left(\frac{S - r}{S - R} \right)^3 \quad (4.21)$$

Substituting equation (4.21) in the first term on the left side of equation (4.10) and simplifying we get

$$M = \frac{3\rho}{(S - R)^3} \left[\frac{S^6}{60} + \frac{R^6}{6} - \frac{3R^5S}{5} + \frac{3R^4S^2}{4} - \frac{R^3S^3}{3} \right] \quad (4.22)$$

Substituting equation (4.22) in the diffusion equation (equation (4.10)) we get

$$C_S = \frac{\rho_g R^3 - \rho_{g0} R_0^3 + MC_W - \rho C_0 (S^3 - R^3)}{M - \rho (S^3 - R^3)} \quad (4.23)$$

The interfacial mass balance equation becomes after substituting equation (4.21)

$$\frac{d}{dt} (\rho_g R^3) = \frac{9\rho D R^2}{(S - R)} (C_S - C_W) \quad (4.24)$$

Converting the expression for M into dimensionless form using the dimensionless parameters shown in Table (3.1) we have

$$M = \frac{3\rho R_0^3}{(S^* - R^*)^3} \left(\frac{S^{*6}}{60} - \frac{S^{*3}R^{*3}}{3} + \frac{3S^{*2}R^{*4}}{4} - \frac{3R^{*5}S^*}{5} + \frac{R^{*6}}{6} \right) \quad (4.25)$$

Substituting parameters from Table (3.1) equation (4.24) becomes

$$\frac{d\xi^*}{dt^*} = \frac{9R_g T \mu \rho D}{R_0^2 P_a^2 P_{g0}^*} \frac{R^{*2}}{(S^* - R^*)} (C_S - C_W) \quad (4.26)$$

The rest of the procedure for modifying the equations is the same as that shown for second order profile solution.

Alternate simplification

Another approach to simplifying the second term in equation (4.7) is to assume that the velocity of the liquid inside the shell (v_r) is negligibly small.

$$\frac{d}{dt} \left(\frac{C_S R^3}{3} \right) = \frac{R^3}{3} \frac{dC_S}{dt} + r^2 v_r C_S \quad (4.27)$$

If we let $v_r = 0$ during this part of the time we have

$$\frac{d}{dt} \left(\frac{C_S R^3}{3} \right) = \frac{R^3}{3} \frac{dC_S}{dt} \quad (4.28)$$

Substituting in the diffusion equation expression we have

$$\int_R^S (C_A - C_S) r^2 dr + \frac{S^3}{3} (C_S - C_0) - \frac{C_S R^3 - C_0 R_0^3}{3} = -\frac{1}{3\rho} (\rho_g R^3 - \rho_{g0} R_0^3) \quad (4.29)$$

dividing equation (4.29) by $C_W - C_S$, which is a function of time only we get

$$\int_R^S \frac{(C_A - C_S)}{(C_W - C_S)} r^2 dr + \frac{S^3}{3} \frac{(C_S - C_0)}{(C_W - C_S)} - \frac{C_S R^3 - C_0 R_0^3}{3(C_W - C_S)} = \frac{1}{3\rho} \frac{\rho_g R^3 - \rho_{g0} R_0^3}{(C_S - C_W)} \quad (4.30)$$

Evaluating the above expression after substitution and extracting the expression for C_S

$$C_S = \frac{\rho_g R^3 - \rho_{g0} R_0^3 + M C_W - \rho C_0 (S^3 - R_0^3)}{M - \rho (S^3 - R^3)} \quad (4.31)$$

The only difference between the equation (4.13) and equation (4.31) is that in the last term of the numerator. Equation (4.31) has R_0 in the last term of the numerator, but equation (4.13) has the instantaneous bubble radius R . Converting equation (4.31) into dimensionless form we get

$$C_S = \frac{MK_h P_a P_g^* - \rho K_h P_a P_{g0}^* R_0^3 (S^{*3} - 1) + \frac{P_a R_0^3 P_{g0}^* \xi^*}{R_g T}}{M - \rho R_0^3 (S^{*3} - R^{*3})} \quad (4.32)$$

The rest of the procedure to solve the equations is the same that used when the assumption of $\frac{S^3 - R^3}{3} = \text{constant}$, was used. The boundary conditions for this set of equations are

$$R^*(0) = 1.0 \quad (4.33)$$

$$\zeta^*(0) = 0 \quad (4.34)$$

The momentum equation (equation (4.4)) and the reduced mass balance equation (equation (4.19)) need to be solved simultaneously subject to the boundary equations. Either equation (4.18) or equation (4.32) can be used to substitute for C_S in equation (4.19).

Second approach

In this approach global mass balance is also instead of just the interfacial mass balance.

The global mass balance at any instant of time can be written as:

$$M_{gb} + M_{gs} = M_{g\text{initial}} \quad (4.35)$$

Where

M_{gb} = Mass of gas inside the bubble

M_{gs} = Mass of gas inside the liquid shell

$M_{g\text{initial}}$ = Mass of gas initially i.e., at time $t = 0$

$$M_{\text{ginitial}} = \frac{4}{3}\pi(S_0^3 - R_0^3)C_0\rho \quad (4.36)$$

$$M_{\text{gb}} = \frac{4}{3}\pi R^3 \frac{C_W}{K_h A} \quad (4.37)$$

At this point the concentration of gas inside the liquid shell can be approximated in two different ways

1) If C_S is assumed as the concentration inside the shell we get

$$M_{\text{gs}} = \frac{4}{3}\pi(S_0^3 - R^3)C_S\rho \quad (4.38)$$

Substituting in the mass balance equation and extracting C_S we get

$$C_S = \frac{S^3 - R_0^3}{S^3 - R^3}C_0 - \frac{R^3}{S^3 - R^3} \frac{C_W}{K_h A \rho} \quad (4.39)$$

2) If the average of C_S , C_W is assumed as the concentration of the gas inside the shell.

We get

$$M_{\text{gs}} = \frac{4}{3}\pi(S_0^3 - R^3) \frac{C_S + C_W}{2} \rho \quad (4.40)$$

Equation (4.40) is obtained by substituting $\frac{C_S + C_W}{2}$ for the concentration of the gas

inside the shell. Substituting in the mass balance equation and extracting C_S we get

$$C_S = \frac{2C_0(S^3 - R_0^3)}{S^3 - R^3} - \frac{2C_W R^3}{K_h A \rho (S^3 - R^3)} - C_W \quad (4.41)$$

Instead if the exact expression for mass of gas inside the shell is used we have

$$M_{\text{gs}} = 4\pi\rho \int_R^S C_A r^2 dr \quad (4.42)$$

Substituting in the mass balance equation (equation (4.35)) and extracting C_S we get

$$C_S = \frac{\frac{S^3 - R_0^3}{3} C_0 - \frac{C_W R^3}{3K_h A \rho} - \frac{C_W}{(S-R)^2} \left(\frac{S^5}{30} - \frac{S^2 R^3}{3} + \frac{S R^4}{2} - \frac{R^5}{3} \right)}{\frac{S^3 - R^3}{3} - \frac{1}{(S-R)^2} \left(\frac{S^5}{30} - \frac{S^2 R^3}{3} + \frac{S R^4}{2} - \frac{R^5}{3} \right)} \quad (4.43)$$

From equation (4.14) we have

$$C_S = \frac{\rho_g R^3 - \rho_{g0} R_0^3 + M C_W - \rho C_0 (S^3 - R_0^3)}{M - \rho (S^3 - R^3)} \quad (4.44)$$

Equating equation (4.43) and equation (4.44) we get an expression for C_W

$$C_W = \frac{C_0 \left(\frac{R_0^3}{K_h A} + \rho (S^3 - R_0^3) + 2 \frac{S^3 - R_0^3}{S^3 - R^3} (M - \rho (S^3 - R^3)) \right)}{\left(\frac{R^3}{K_h A} + \frac{2 R^3 (M - \rho (S^3 - R^3))}{K_h A \rho (S^3 - R^3)} \right) + 2 M - \rho (S^3 - R^3)} \quad (4.45)$$

The momentum equation in dimensionless form is

$$\frac{4(C_2 + 1 - R^{*3})}{1 + C_2} R^* = \frac{C_W R^*}{K_h P_a} - P_f^* R^* - C_3 \quad (4.46)$$

C_W can be substituted from equation (4.45). We have just one equation (equation (4.46)) involving the dependent variable, the non-dimensional radius of the bubble. This equation can be solved using the boundary condition:

$$R^*(0) = 1 \quad (4.47)$$

Only one boundary condition is required, as the momentum equation has been simplified to a first order equation in R^* .

Third approach

This approach uses the momentum equation along with the mass balance equations, both interfacial and overall, to evaluate the profiles. This approach does not use the Fick's law of diffusion equation explicitly. Using the average of C_S , C_W as the concentration of the gas inside the shell we obtain the following expression for C_S

$$C_S = \frac{2C_0(S^3 - R_0^3)}{S^3 - R^3} - \frac{2C_W R^3}{K_h A \rho (S^3 - R^3)} - C_W \quad (4.48)$$

The interfacial mass-balance equation involves the gradient of concentration, C_A at the bubble wall, which can be expressed as

$$\left. \frac{\partial C_A}{\partial r} \right|_{r=R} = -\frac{2(C_W - C_S)}{S - R} \quad (4.49)$$

Equation (4.49) is obtained by differentiating equation (4.21) with respect to the radial coordinate r . Substituting equation (4.49) in the interfacial mass-balance (equation (3.17)) and converting into dimensionless form using parameters from Table (3.1), we have

$$C_S - C_W = \left(\frac{2C_0(S^{*3} - 1)}{S^{*3} - R^{*3}} - \frac{2C_W R^{*3}}{K_h A \rho (S^{*3} - R^{*3})} - 2C_W \right) \quad (4.50)$$

Because of non-linearity encountered in the differential equation when C_W is used, we use the transformation

$$C_W = \frac{P_{g0}^* \left(1 + \sqrt{\zeta^*} \right) K_h P_a}{R^{*3}} \quad (4.51)$$

$$\frac{d\xi^*}{dt^*} = \frac{6R_g T \mu \rho D}{R_0^2 P_a^2 P_{g0}^*} \frac{R^{*2}}{(S^* - R^*)} (C_S - C_W) \quad (4.52)$$

Equation (4.52) can also be written as

$$\frac{d\zeta^*}{dt^*} = 2\sqrt{\zeta^*} (6C_4C_5) \left(\frac{R^{*2}}{S^* - R^*} \right) (C_S - C_W) \quad (4.53)$$

$C_S - C_W$ can be substituted from the equation (4.50) into equation (4.53). Now equations (4.53) can be solved along with the momentum equation (equation (4.4)) for a finite shell.

The boundary conditions for this set of equations are

$$R^*(0) = 1 \quad (4.54)$$

$$\zeta^*(0) = 0 \quad (4.55)$$

Complete solution

Arefmanesh obtained complete profile by solving the diffusion, momentum and mass-balance equation in its entirety [1]. The procedure used by Arefmanesh is shown in this section. To solve for the concentration profile, the diffusion equation (equation (3.13)) is transferred to the Lagrangian coordinate which eliminates the convective term. The Lagrangian coordinate transformation, which is widely used in phase phenomenon, is defined as

$$y = r^3 - R^3(t) \quad (4.56)$$

$$t' = t \quad (4.57)$$

where (r, t) and (y, t') are the old and new coordinates respectively. To transfer the diffusion equation, time and special derivatives are needed in the new coordinate system.

Using the chain rule of differentiation, the following equation are obtained

$$\frac{\partial}{\partial r} = \frac{\partial}{\partial y} \frac{\partial y}{\partial r} + \frac{\partial}{\partial t'} \frac{\partial t'}{\partial r} \quad (4.58)$$

$$\frac{\partial}{\partial t} = \frac{\partial}{\partial y} \frac{\partial y}{\partial t} + \frac{\partial}{\partial t'} \frac{\partial t'}{\partial t} \quad (4.59)$$

Substituting these expressions into the above equations, results in the following transformations

$$\frac{\partial}{\partial t} = \frac{\partial}{\partial t'} - 3R^2 \dot{R} \frac{\partial}{\partial y} \quad (4.60)$$

$$\frac{\partial}{\partial r} = 3r^2 \frac{\partial}{\partial y} \quad (4.61)$$

Using the above transformation, equation (3.13) is transferred to the Lagrangian coordinate system. The diffusion equation in the new coordinate system is given by

$$\frac{\partial C'_A}{\partial t} = 9D \frac{\partial}{\partial y} \left(\left(y + R^3 \right)^{\frac{4}{3}} \frac{\partial C'_A}{\partial y} \right) \quad (4.62)$$

It is assumed that there is no gas diffusion at the outer boundary of the liquid shell. Mathematically, this implies that the concentration gradient at the outer boundary of the shell is equal to zero at all times. Hence, the boundary conditions for equation (4.62) written in terms of the new coordinate system are as follows

$$C'_A|_{y=0} = k_h (P_g - P_{g0}) \quad (4.63)$$

$$\left. \frac{\partial C'_A}{\partial y} \right|_{(y=S^3-R^3)} = 0 \quad (4.64)$$

and as the initial concentration is equal to C_0 ,

$$C'_A|_{t=0} = 0 \quad (4.65)$$

At the early stage of the bubble growth, the concentration gradient close to the interface is quite large which makes the task of obtaining numerical solution to equation (4.62)

difficult. To overcome this difficulty, a vector field Ω with the components C'_A and

$9D(y + R^3)^{\frac{4}{3}} \frac{\partial C'_A}{\partial y}$ in the $y - t$ plane is introduced. Using equation (4.62), it can be shown

that such a vector field is irrotational. Therefore, following the properties of the irrotational fields, there exists a potential function $\Phi(y, t)$ such that

$$\Omega = \nabla \Phi \quad (4.66)$$

This allows one to recast the diffusion equation (equation (4.62)) in terms of the potential function. The resulting equation is given by

$$\frac{\partial \Phi}{\partial t} = 9D(y + R^3)^{\frac{4}{3}} \frac{\partial^2 \Phi}{\partial y^2} \quad (4.67)$$

where $\frac{\partial \Phi}{\partial y}$ is equal to C'_A . The initial and boundary conditions given by equations (4.63),

(4.64) and (4.65) are also written in terms of the new dependent variable (Φ) as follows

$$\Phi(y, 0) = 0 \quad (4.68)$$

$$\Phi(y = 0, t) = K_h (P_g - P_{g0}) \quad (4.69)$$

$$\Phi_{yy}(y = S^3 - R^3, t) = 0 \quad (4.70)$$

The variable $\Phi(y, t)$ is the integral of the gas concentration with respect to the y coordinate and varies more smoothly near the interface. Hence the solution of $\Phi(y, t)$ in the transformed equation (equation (4.67)) poses less numerical difficulties and is more efficient during the early stages of the bubble growth when there is a large variation in the concentration gradient [1].

Equations (3.17), (4.2), (4.67), (4.68), (4.69) and (4.70) constitute the system of the governing equations and the boundary conditions for the growth of a spherical bubble surrounded by a shell of Newtonian liquid finite thickness. Initial conditions for equations (3.17) and (4.2) are

$$P_g(t = 0) = P_{g0} \quad (4.71)$$

$$R(t = 0) = R_0 \quad (4.72)$$

Then these set of equations were solved using Fourth-order Runge-Kutta method for solving differential equations [1].

Numerical evaluation

The results presented in this study are confined to highly viscous liquids such as polymer melt. To estimate the magnitude of the inertia terms in the momentum equation (4.2), an order of magnitude analysis was conducted on this equation. To make the terms of the order of one, the equilibrium radius (R_e) and the initial gas pressure were used to non-

dimensionalize equation (4.2). This resulted in the dimensionless number $\left(\frac{\rho R_e^2 P_{g0}}{\eta^2} \right)$,

which can be regarded as a Reynolds number. For typical values of $\rho = 10^3 \text{ kg/m}^3$, $R_e = 1 \text{ mm}$, $P_{g0} = 10^6 \text{ N/m}^2$ and $\eta = 10^3 \text{ N.s/m}^2$, the magnitude of this number is of the order of 10^{-3} , which is much smaller than unity. Therefore, for highly viscous liquids, the role of inertia terms in the growth process can be safely neglected.

The system of differential equations governing the bubble growth is non-linear and coupled for which there does not exist any known analytical solution. Mathematica 4.1 was used to solve the coupled differential equations. A fourth-order Runge-Kutta method was used to solve the differential equations. In some of the evaluations there was a problem in getting the solver started due to singularity of ζ^* at time $t = 0$. Therefore a non-zero value of ζ^* was specified for example 10^{-6} . When a non-zero value of ζ^* was chosen the solution was obtained. In order to check the dependency of ζ^* on the initial value chosen, the initial values were varied from 10^{-3} to 10^{-7} . No significant change in the results was obtained by choosing any value between 10^{-3} to 10^{-7} . Arefmanesh solved the complete concentration profile by solving the three coupled governing equations (3.17, 4.2 and 4.67) using a combination of the Runge-Kutta method and the explicit finite difference scheme [1].

The numerical simulation was used to investigate the effect of various dimensionless parameters such as C_2, C_3, C_4 and the initial gas concentration on the bubble growth. A large range of values was used in the simulation. The lower and upper bound of these parameters are given in Table (4.2).

Table 4.2: Lower and upper bounds for dimensionless variables C_2, C_3 and C_4

	Lower Bound	Upper Bound
C_2	10^4	10^8
C_3	0.3	0.9
C_4	10	10^4

Equilibrium calculations

The equilibrium bubble radius can be evaluated by applying a mass balance to the dissolved gas in the liquid around the bubble. The calculated equilibrium radius may then be compared to the predicted value from the numerical solution of the governing equations to verify the accuracy of the numerical predictions. The conservation of mass for the dissolved gas in the liquid and the ideal gas law for the gas inside the bubble are used to evaluate the equilibrium bubble radius. The bubble radius R_e and the gas pressure inside the bubble P_{ge} at the equilibrium are related through the following equation

$$P_{ge} = P_f + \frac{2\sigma}{R_e} \quad (4.73)$$

The equilibrium gas concentration C_e is related to the equilibrium gas pressure through Henry's law ($C_e = K_h P_{ge}$). The ideal gas law for the gas inside the bubble at the equilibrium gives

$$P_{ge} V_e = M_{ge} R_g T_e \quad (4.74)$$

where V_e is the bubble volume at the equilibrium and is equal to $\frac{4}{3}\pi R_e^3$. R_g is the ideal gas constant. T_e is the equilibrium temperature of the gas inside the bubble, which is assumed to be the same as the polymer temperature. M_{ge} is the mass of the gas inside the bubble at the equilibrium and is equal to $(4/3)\pi(S_0^3 - R_0^3)\rho(C_0 - C_e)$. Substituting these expressions into the ideal gas equation (equation (4.74)), results in the following expression for the equilibrium bubble radius

$$\left(P_f + \frac{2\sigma}{R_e}\right) \left(\frac{4}{3}\pi R_e^3\right) = \frac{4}{3}\pi(S_0^3 - R_0^3) \rho \left(C_0 - K_h \left(P_f + \frac{2\sigma}{R_e}\right)\right) R_g T_g \quad (4.75)$$

The equilibrium bubble radius is obtained by solving equation (4.75). The equilibrium radius obtained by solving the coupled differential equations matches well with the equilibrium radius obtained from equation (4.75).

Comparison of profiles

A variety of cases have been studied by varying the parameters C_2 , C_4 and P_{g0}^* . C_2 represents the thickness of the liquid shell. The larger the value of C_2 , the bigger the liquid shell and the infinite shell approximation become more valid. The parameter C_4 is indicative of the diffusion coefficient of the gas in the liquid. The higher the value of C_4 , the higher the diffusion rate. The initial gas pressure P_{g0}^* was also varied and the radius profiles studied. The value of the initial gas pressure P_{g0}^* was limited to 15. Higher initial gas pressures were not chosen because they are seldom observed in practical situations and may also violate ideal gas law.

Figures (4.2), (4.3) and (4.4) show the effect of thickness of the liquid shell (parameter C_2) enveloping the bubble on the bubble growth. The three different values of C_2 (10^4 , 10^6 and 10^8) correspond to thin, medium and thick shells. The results show that as the thickness of the liquid shell enveloping the bubble increases, the time to reach equilibrium increases. Also, since the mass of the gas within the shell increases with its thickness, the value of the equilibrium radius will be larger. At the onset of the growth,

the various solutions match well with the complete solution obtained by Arefmanesh [1]. More so the 'method 3' method matches very well with the complete solution. The equilibrium radii predicted by the various methods are varying slightly from the complete solution. It can be seen that the 'method 1' predicts the equilibrium radius very well compared to the other methods. The 'method 1', 'method 3' under-predict the initial growth rate, but the growth rate picks up finally and the 'method 1' predicts the final equilibrium radius very closely to the complete equilibrium radius. The 'method 3', 'method 2' and 'Infinite medium' solutions over-predict the final equilibrium radius by about 10-15 %. The polynomial profile solutions for infinite medium of liquid surrounding the bubble severely over-predict the final equilibrium radius. Also from Figures (4.5) and (4.6), there is no appreciable difference between the second order and third order polynomial profile solutions as far as the final equilibrium radius is predicted. But as the order of the profile increases the accuracy increases slightly. The relative error between the final equilibrium radius decreases as the shell thickness increases.

Figures (4.2), (4.7), and (4.8) demonstrate the effects of the diffusion coefficient on the growth dynamics by changing the value of the parameter C_4 . An increase in diffusion coefficient accelerates the diffusion process. Therefore, the bubble radius attains its equilibrium faster. For the case of using polynomial profiles for an infinite medium, increasing the diffusion coefficient results in a higher growth rate throughout the period. Therefore they overestimate the growth rate significantly as seen from the figures. The error decreases as the diffusion coefficient is decreased. Comparing the polynomial profile solutions for the case of finite thickness shells we can see that the error decrease

with increasing diffusion coefficient. All the profiles match well with the complete solution for $C_4 = 10^4$. However the profiles are slightly different for the case of $C_4 = 10^2$. All the finite shell methods predict the final equilibrium radius within 13 % of that predicted by complete method. The 'method 3' predicts the bubble growth behavior well for times t^* less than two-thirds the time taken to reach equilibrium. At the end of the growth process the radius profile for complete and 'method 3' diverges and reach different equilibrium radius.

The influence of initial gas concentration P_{g0}^* on the growth is depicted in Figs. (4.2), (4.4) and (4.10). The results are for three different values of the dimensionless initial gas pressure of 5, 10, and 15, which are related to the initial gas concentration through Henry's Law. Higher initial gas pressures were not chosen because they may violate the ideal gas law and because they are seldom observed in practical situations. Higher initial gas pressure results in higher growth rate and also a higher final equilibrium radius.

From the results it can be seen that the profile solutions for high initial gas pressure and high diffusivity give good results. It can also be seen that the models do not work well for low gas pressure, low gas diffusivity and for thick shells. However the models developed using 'method 1' and 'method 3' predict the bubble growth better than the infinite medium solution. The reasons for better profile prediction during high initial gas pressure and high diffusivity are that the concentration boundary layer reaches the outer shell very fast, and profile switching is not necessary. However for thick shells, low initial gas

pressure and low gas diffusivity the concentration boundary layer takes considerable time to reach the outer edge. Therefore we need to use profile switching in these cases to better predict the bubble growth. This profile switching can be done using “Penetration Depth” techniques [31].

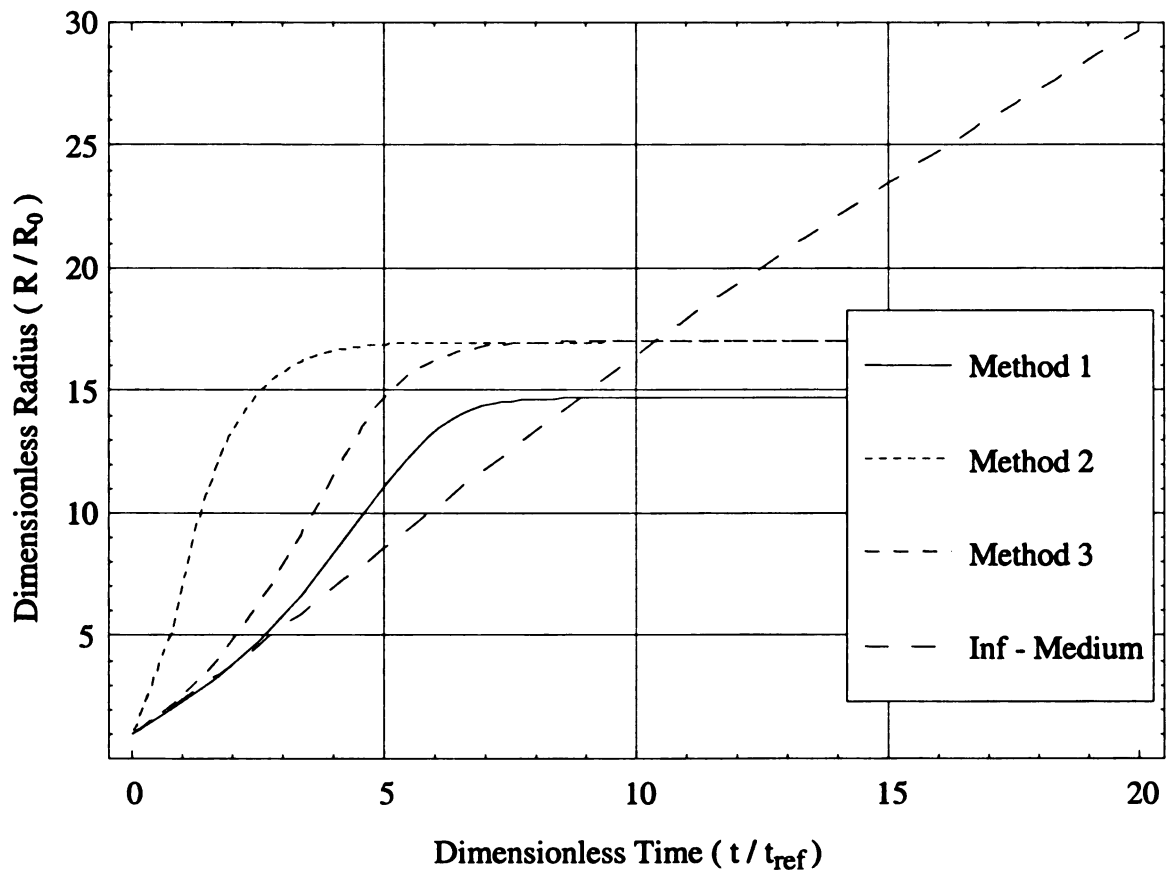


Figure 4.2: Comparison between various methods of evaluating the radius profiles for low thickness shell ($C_2 = 10^4$), $C_3 = 0.4$, $C_4 = 10^2$ (average gas diffusivity) and initial gas pressure $P_{g0}^* = 10$.

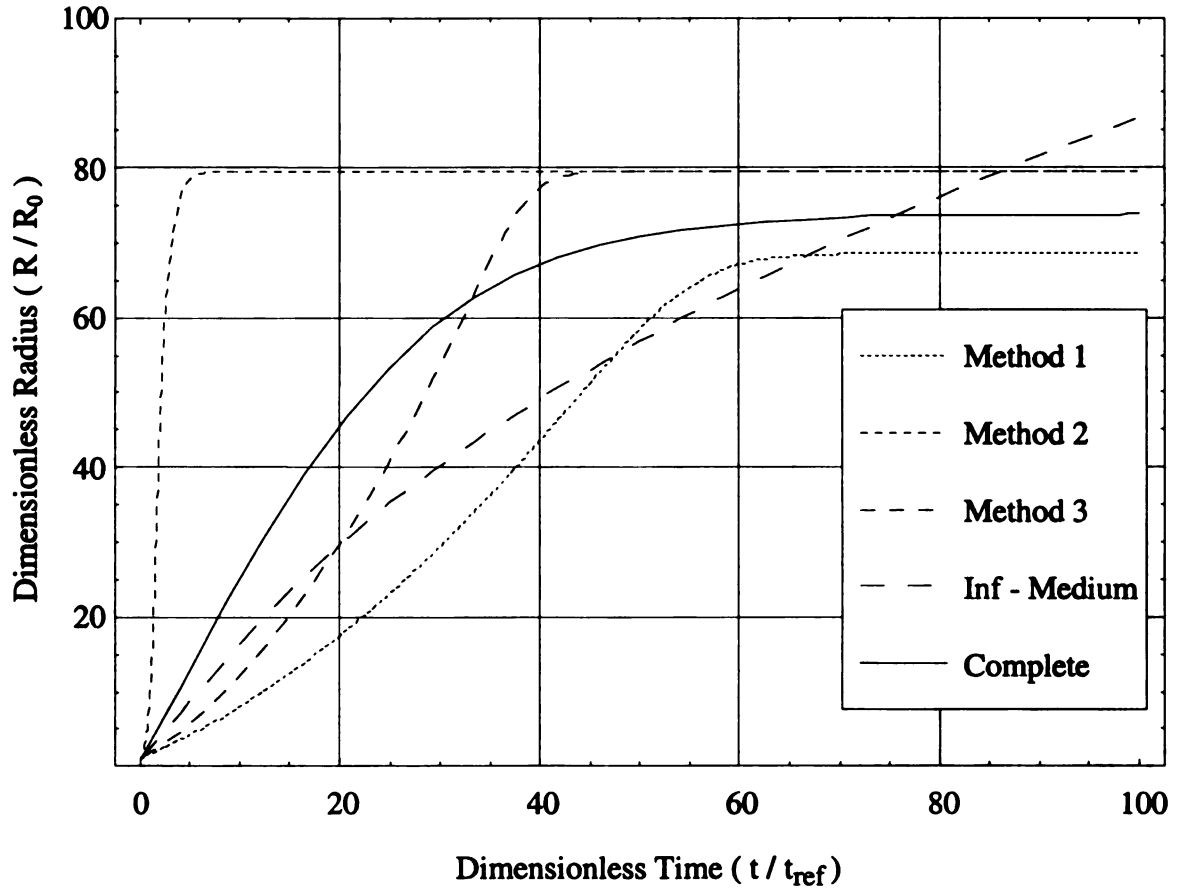


Figure 4.3: Comparison between approximate and accurate numerical solutions for medium thickness shell ($C_2 = 10^6$), $C_3 = 0.4$, $C_4 = 10^2$ (average gas diffusivity) and $P_{g0}^* = 10$.

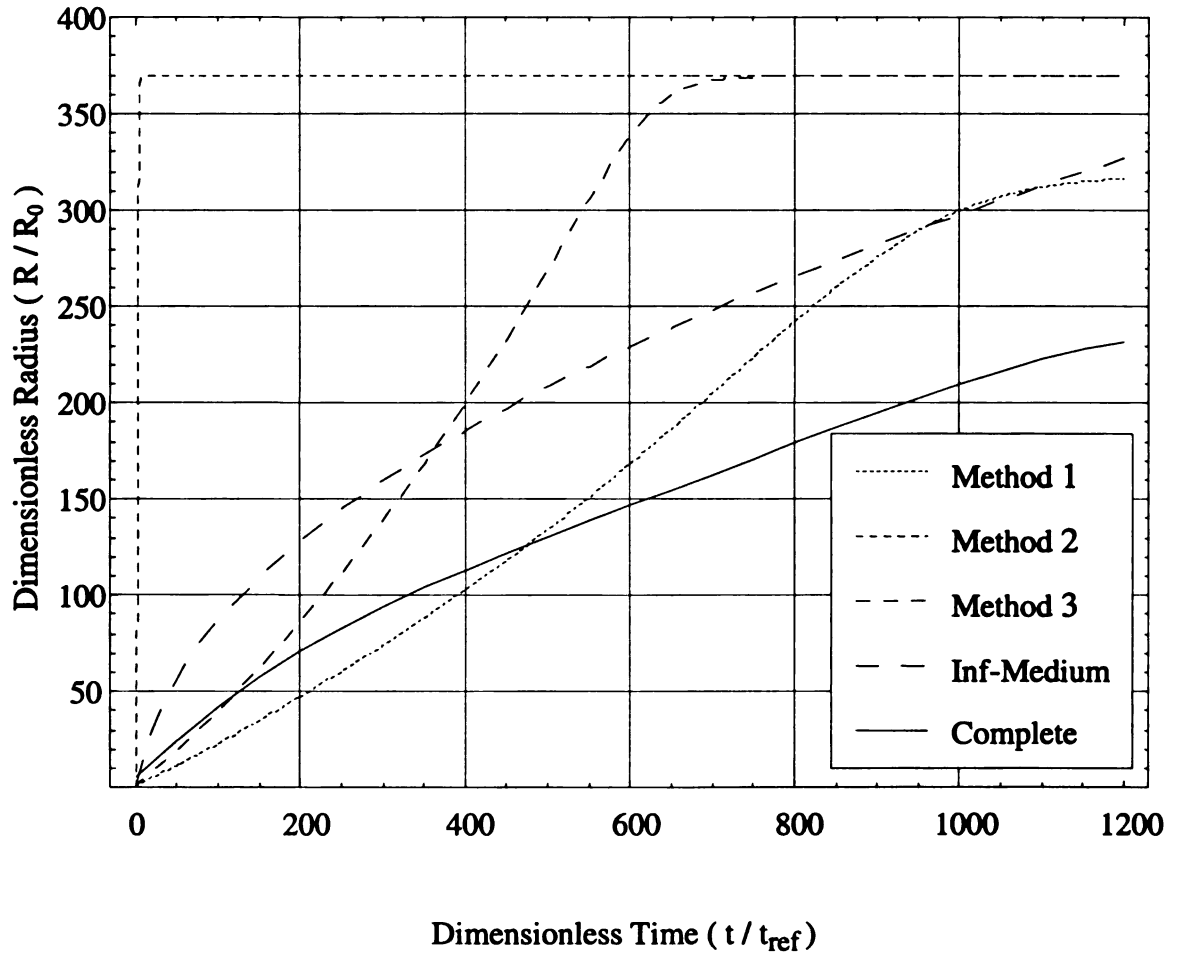


Figure 4.4: Comparison between approximate and accurate numerical solutions for high thickness shell ($C_2 = 10^8$), $C_3 = 0.4$, $C_4 = 10^2$ (average gas diffusivity) and $P_{g0}^* = 10$.

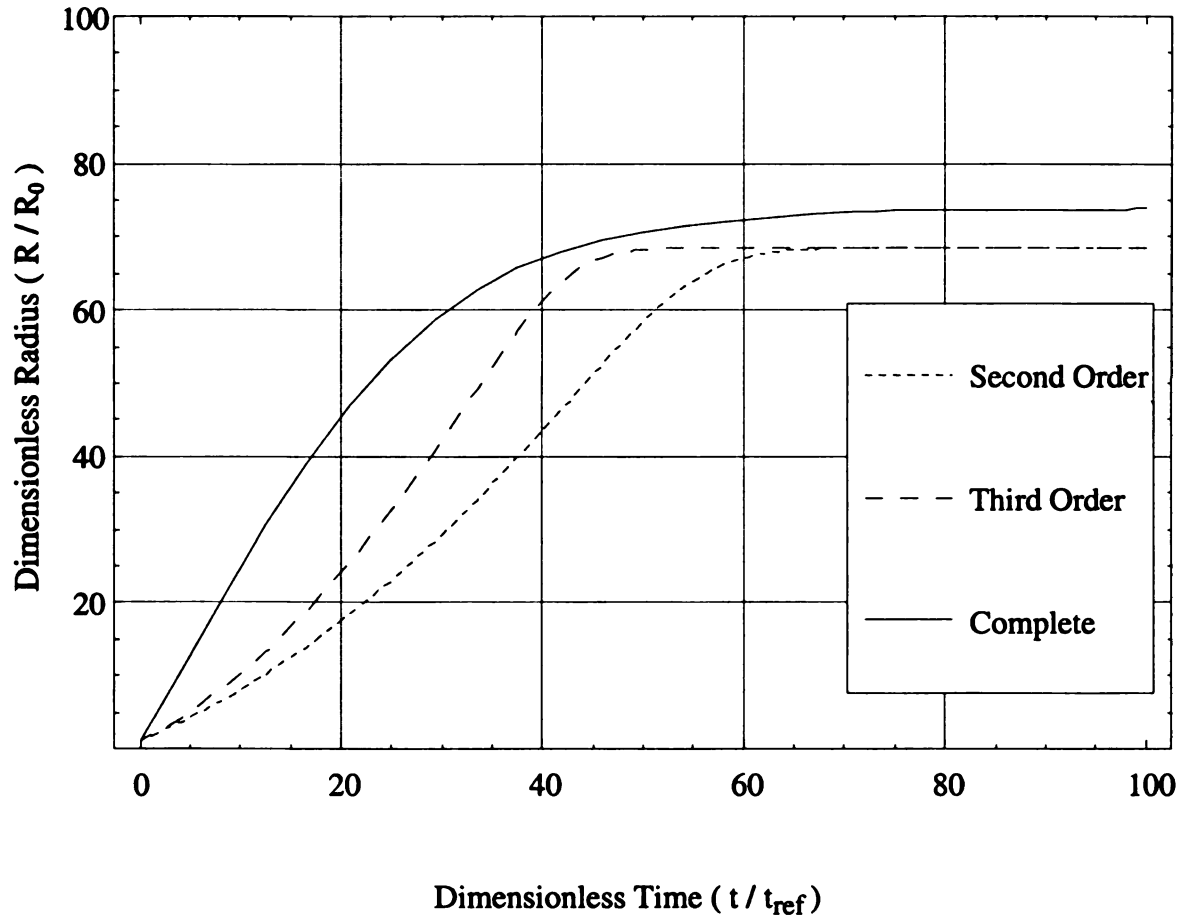


Figure 4.5: Comparison between second, third order profile solutions using ‘method 1’ and the complete solution obtained by Arefmanesh [1] for medium thickness shell ($C_2 = 10^6$), $C_3 = 0.4$, $C_4 = 10$ (average gas diffusivity) and initial gas pressure $P_{g0}^* = 10$.

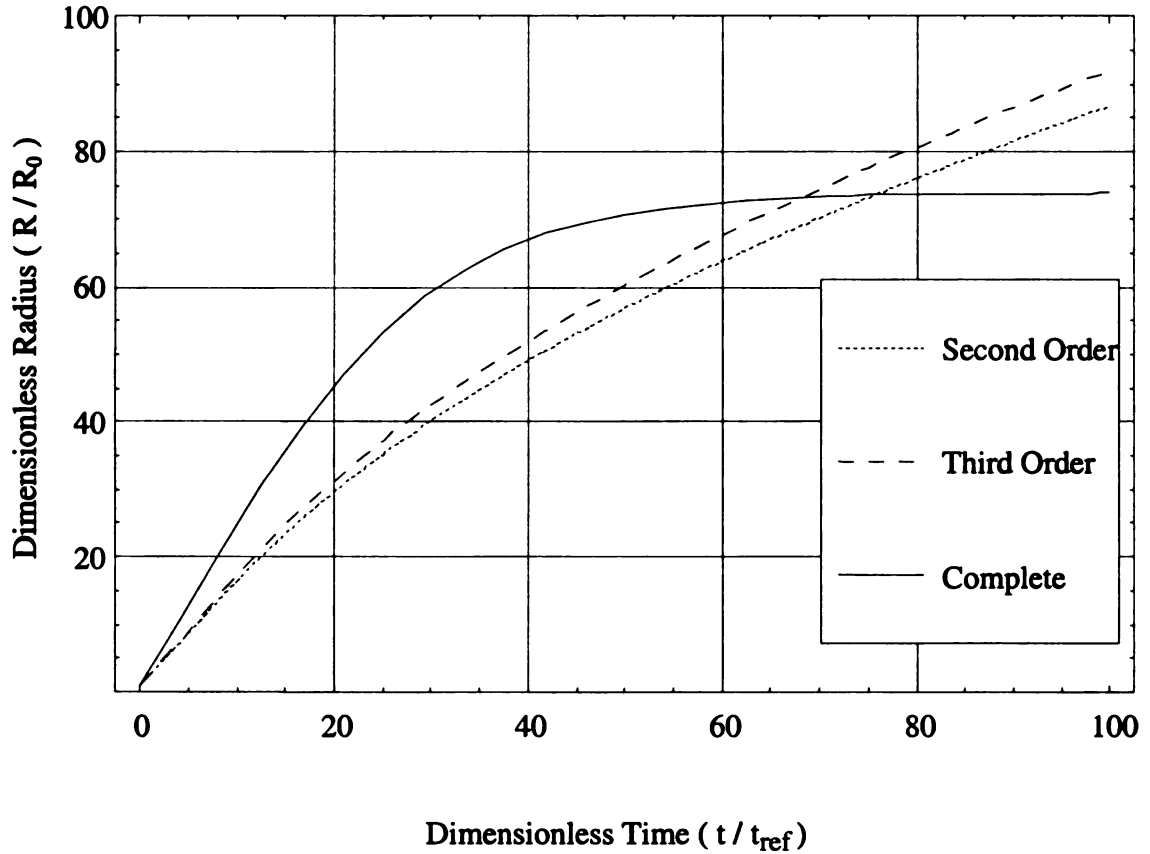


Figure 4.6: Comparison between second order, third order polynomial profile solutions for infinite medium and complete solution obtained by Arefmanesh [1] for medium thickness shell ($C_2 = 10^6$), $C_3 = 0.4$, $C_4 = 10$ (average gas diffusivity) and initial gas pressure $P_{g0}^* = 10$.

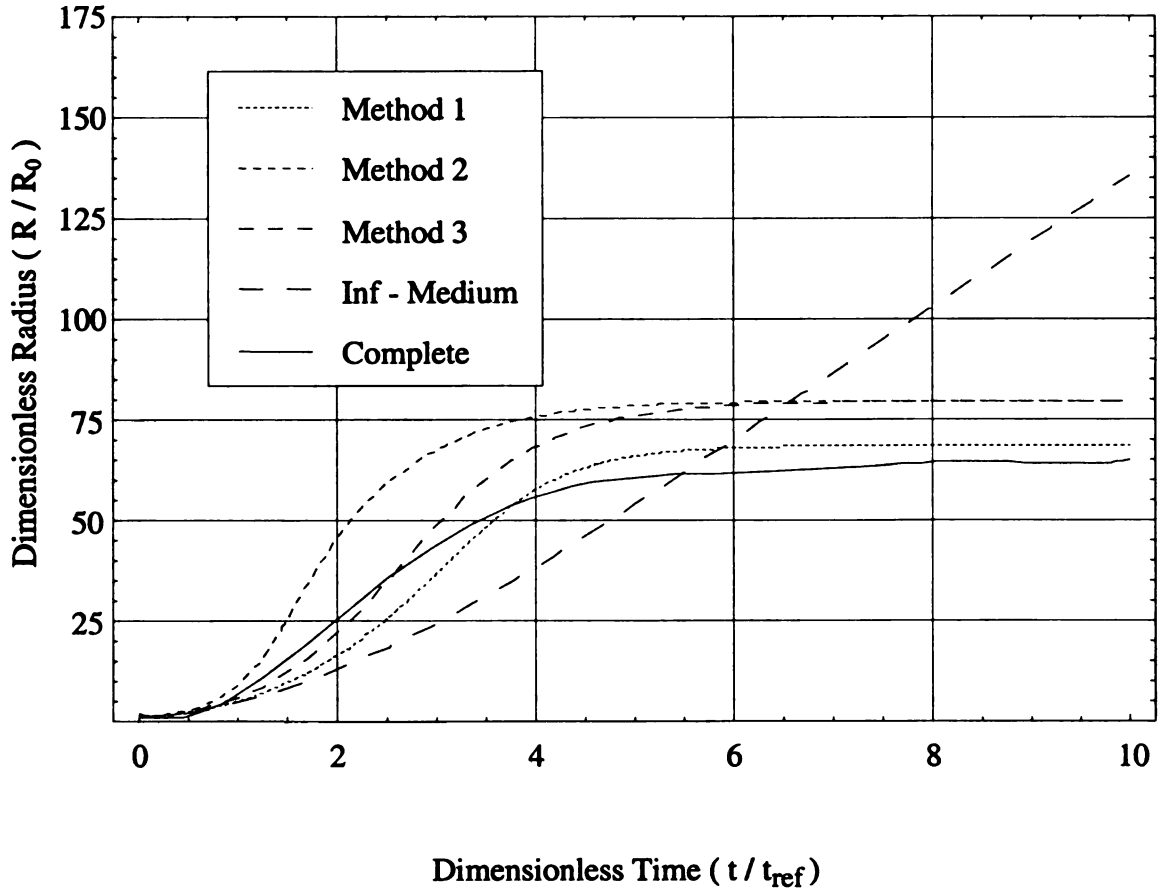


Figure 4.7: Comparison between approximate and accurate numerical solutions for medium thickness shell ($C_2 = 10^6$), $C_3 = 0.4$, $C_4 = 10^4$ (High gas diffusivity) and initial gas pressure $P_{g0}^* = 10$.

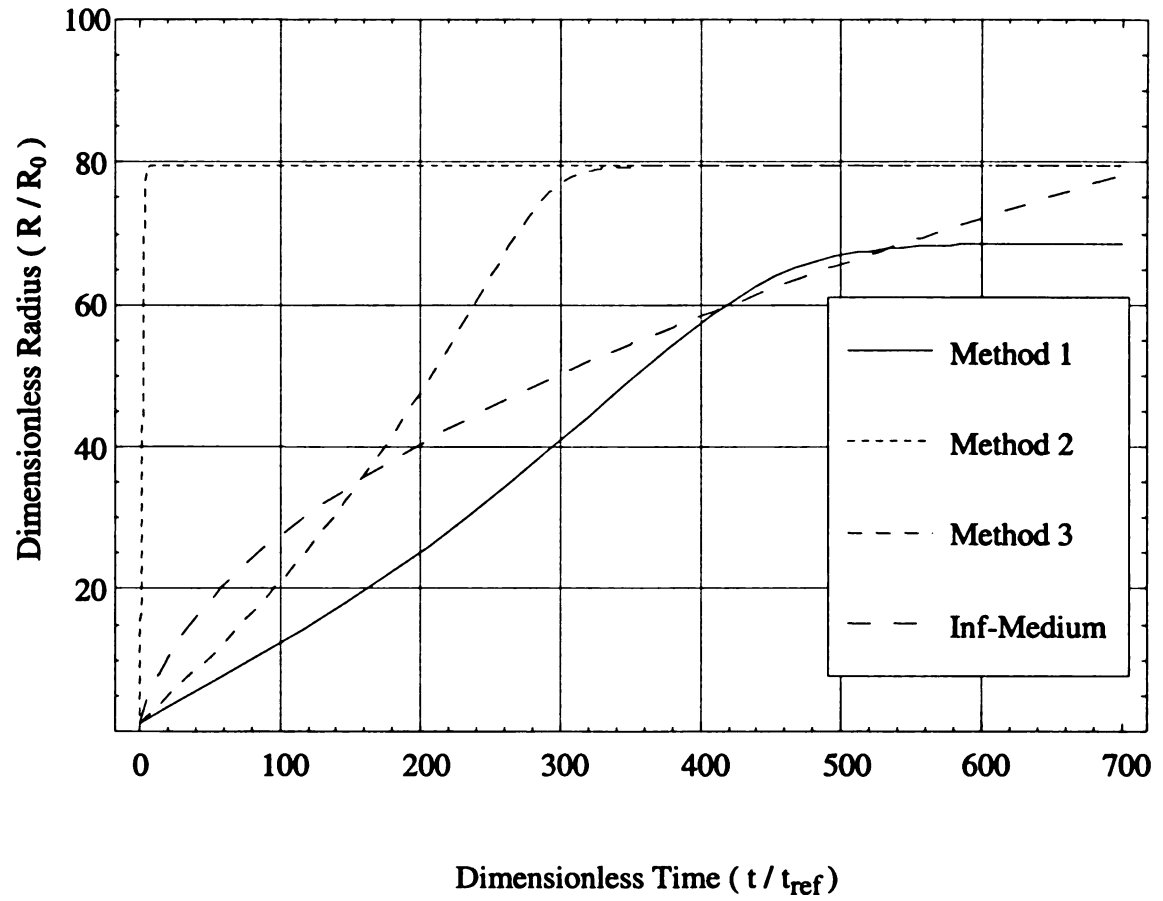


Figure 4.8: Comparison between various methods of evaluating the radius profiles for medium thickness shell ($C_2 = 10^6$), $C_3 = 0.4$, $C_4 = 10$ (low gas diffusivity) and initial gas pressure $P_{g0}^* = 10$.

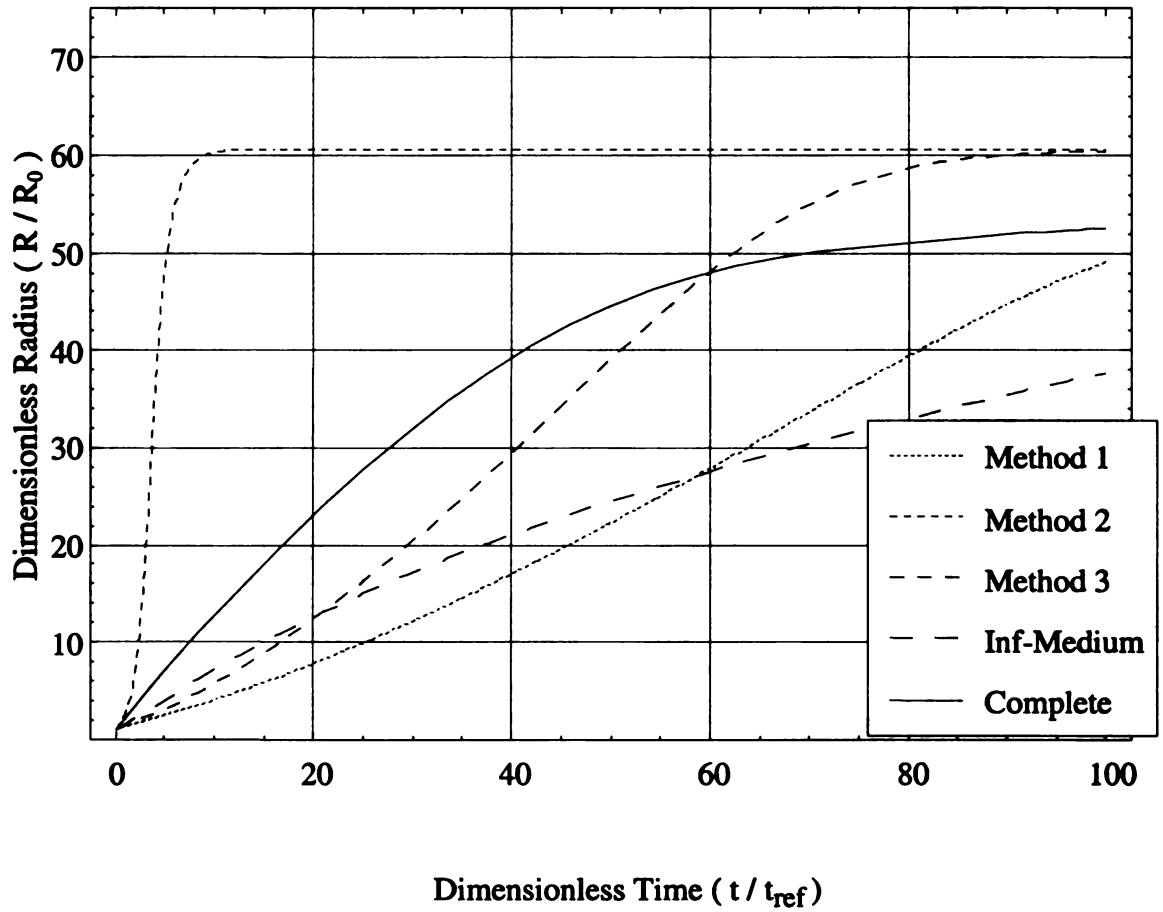


Figure 4.9: Comparison between approximate and accurate numerical solutions for medium thickness shell ($C_2 = 10^6$), $C_3 = 0.4$, $C_4 = 10^2$ (average gas diffusivity) and low initial gas pressure $P_{g0}^* = 5$.

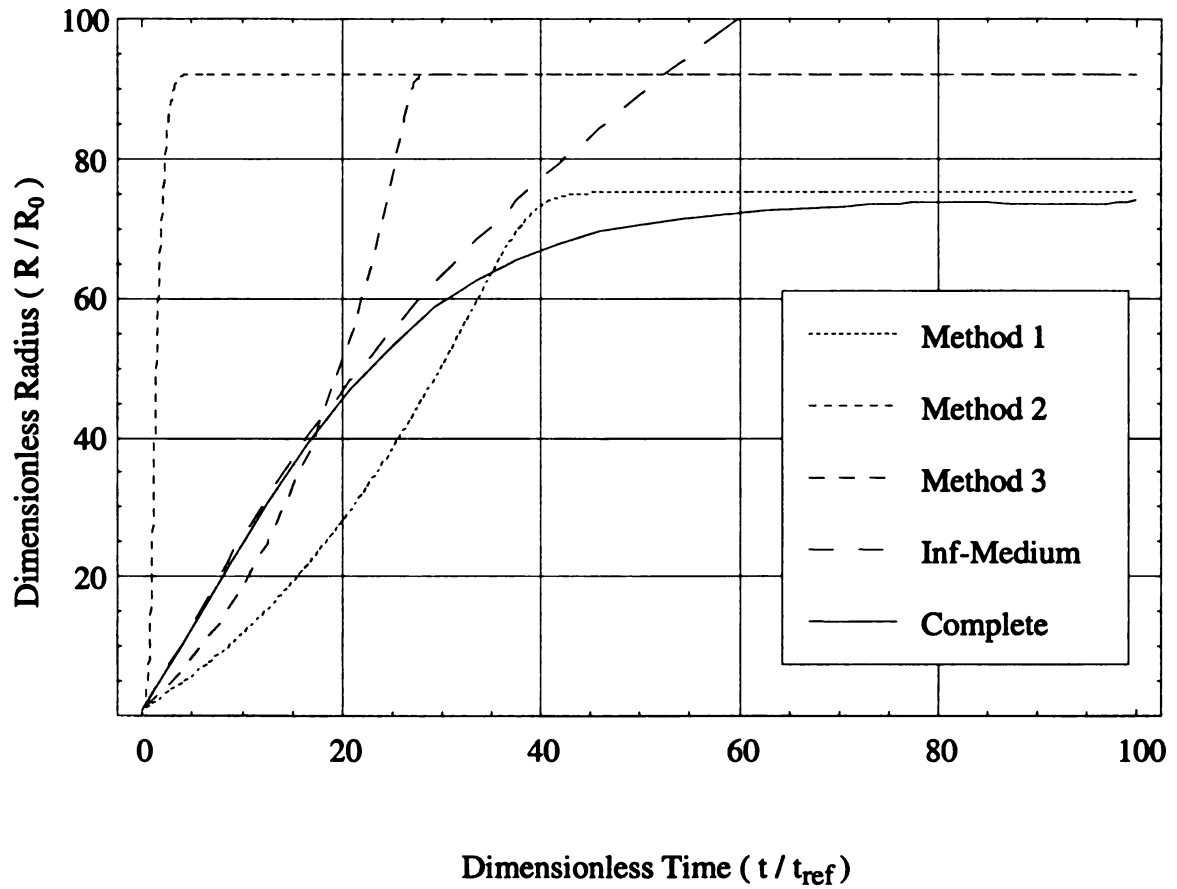


Figure 4.10: Comparison between various methods of evaluating the radius profiles for medium thickness shell ($C_2 = 10^6$), $C_3 = 0.4$, $C_4 = 10^2$ (average gas diffusivity) and initial gas pressure $P_{g0}^* = 15$.

CHAPTER 5

SUMMARY AND CONCLUSIONS

This thesis involves the study of bubble growth in highly viscous liquids. Numerical models for predicting bubble growth in viscous liquids were developed and presented. Numerous researchers have used polynomial profiles approximations for the concentration of the dissolved gas in the liquid to obtain solutions. The same approach has been adopted in this thesis work as polynomial profile approximation lead to easy solutions to predict bubble growth with reasonable accuracy.

The growth of a gas bubble in a liquid containing dissolved gas is due to the simultaneous mass and momentum transfer between the bubble and the liquid. The diffusion of the dissolved gas from the liquid into the bubble is governed by the convection-diffusion equation. A common method to solve the diffusion equation is to assume that concentration gradient is limited to a small boundary close to the bubble interface and use polynomial profiles to describe the gas concentration in the boundary layer. In the first part of the thesis, the governing equations for the growth of a single bubble surrounded by infinite amount of liquid are presented. This approach was first developed by Han and Yoo [26]. In this approach the Integral method was adopted to modify the diffusion equation. The diffusion equation is converted into an integral form. Polynomial profiles are used to approximate the gas concentration in the liquid surrounding the bubble. Second and third order polynomial profiles were used to study the bubble growth. Outside the concentration boundary layer the concentration is assumed to be invariant

and equal to the initial concentration. All derivatives of the concentration are also assumed to be zero outside the boundary layer. This represents the correct physics of the phenomenon for a bubble growing in a shell of liquid with finite amount of dissolved gas only at the initial stage of the bubble growth process. This will depend on the shell thickness, the rapidity at which the growth process occurs, and the initial radius. Near the end of the growth process, when the concentration boundary layer has reached the outer shell, all spatial derivatives of the concentration at the outer boundary of the shell should be equal to zero. However, using this approach the governing equations are reduced to equations (3.10) and (3.26). Then these equations were converted into dimensionless form. These coupled equations were solved using the appropriate boundary conditions.

To incorporate the correct physics of the problem, the bubble growth in a shell of liquid with finite amount of dissolved gas needs to be considered. The governing equations for bubble growth in a shell of liquid were developed. The governing equations are the diffusion equation, conservation of mass equation and momentum transfer equation. The diffusion equation was modified using the 'Integral method'. This involves multiplying the equation with r^2 and integrating over the domain. This technique results in a modified integral diffusion equation. At this point three different approaches were adopted to simplify the diffusion equation.

In the first method it is assumed that the velocity of the liquid surrounding the bubble is negligible. This simplifies the diffusion equation, and assumptions regarding the concentration profile of gas surrounding the bubble were made. The concentration

profiles are assumed to be polynomials. In this study second order and third order polynomial profiles were assumed. The profile equations were substituted into the integrated diffusion equation. The momentum equation and the reduced integral diffusion equation were then converted to dimensionless form and solved using the boundary conditions.

In the second method, apart from the interfacial mass balance equation, the global mass balance equation is also used. Two different expressions for C_s are developed and then equated. This resulted in an expression for C_w , which was substituted into the momentum equation. The momentum equation was then converted to dimensionless form and solved using the appropriate boundary condition.

In the third method the diffusion equation is not used explicitly. The governing equations then are the momentum equation and the interfacial mass balance and global mass balance. The mass balance equations are then combined into one equation and solved along with the momentum equation after converting them into dimensionless form. After these methods the exact method of Arefmanesh [1] was shown. Arefmanesh solved the full diffusion equation without using any approximations for the concentration profile.

A parametric study was conducted and the influence of various dimensionless parameters on the dynamics of the growth was investigated. The results in each case were compared with the approximate solutions obtained using polynomial profiles for gas concentration in infinite medium. They were also compared with the solutions obtained by solving the

full diffusion equation. The parametric study revealed that polynomial profile approximations for gas concentration, to predict the bubble growth behavior are reasonably accurate. These methods also predict the final equilibrium radius very accurately. The approximated solutions using polynomial profiles for bubble growing in an infinite medium over-predict the final equilibrium radius by three to four orders of magnitude.

Further Study

Other ways to solve this kind of problem involve using the “Volumetric Rise” and “Penetration Depth” approaches [31]. In the Volumetric Rise approach the unsteady solution for the flow problem is solved by using scaling. After evaluating the steady state solution using analytical techniques, the unsteady solution is obtained by introducing a scale factor. The scale factor is a function of time only. The unsteady solution is expressed as the product of the steady solution and the scale factor. The success of this method depends on obtaining the steady state solution for the flow problem.

In the Penetration Depth approach the time domain of the problem is divided into two domains. The first time domain is the domain during which the diffusion of mass or momentum has not reached the boundary of the problem. So during this time domain, the diffusion of mass or momentum does not fully affect the whole geometry of the problem. In the second time domain, the diffusion of mass or momentum fully affects the whole geometry of the problem. The solution strategy is to use polynomial profiles which satisfy the boundary conditions of the problem. Then these solution profiles are

introduced in the governing equations solved in the two time domains. At the domain interface the solutions are forced to match. This approach of obtaining solutions to predict the bubble growth behavior is very promising. The solution profiles seem to match in initial stages with the complete solution. This suggests that we need to use the Penetration Depth approach, so that the better profiles can be obtained during the latter stages of the growth.

APPENDIX A

DERIVATION OF INTEGRAL DIFFUSION EQUATION

The diffusion equation in cylindrical coordinate system is

$$\frac{\partial C_A}{\partial t} + V_r \frac{\partial C_A}{\partial r} = D \left[\frac{1}{r^2} \frac{\partial}{\partial r} \left(r^2 \frac{\partial C_A}{\partial r} \right) \right] \quad (\text{A.1})$$

multiplying with r^2 and integrating with respect to r from $r = R$ to $r = S$

$$\int_{r=R}^{r=S} r^2 \frac{\partial C_A}{\partial t} dr + \int_{r=R}^{r=S} r^2 V_r \frac{\partial C_A}{\partial r} dr = D \int_{r=R}^{r=S} d \left[r^2 \frac{\partial C_A}{\partial r} \right] \quad (\text{A.2})$$

as $R^2 \dot{R}$ is a function of time only, it can be brought outside the integral and the expression integrated.

$$\int_{r=R}^{r=S} r^2 \frac{\partial C_A}{\partial t} dr + R^2 \dot{R} (C_S - C_W) = -DR^2 \left(\frac{\partial C_A}{\partial r} \right) \Big|_{r=R} \quad (\text{A.3})$$

using the following transformation

$$y = \frac{R^3}{3} \quad (\text{A.4})$$

we get

$$\int_{y=R^3/3}^{y=S^3/3} \frac{\partial C_A}{\partial t} dy + R^2 \dot{R} (C_S - C_W) = -DR^2 \left(\frac{\partial C_A}{\partial r} \right) \Big|_{r=R} \quad (\text{A.5})$$

Leibnitz's Rule:

$$\int_{a(z)}^{b(z)} \frac{\partial f}{\partial z} dx + f(b(z), z) \frac{\partial b}{\partial z} - f(a(z), z) \frac{\partial a}{\partial z} = \frac{\partial}{\partial z} \int_{a(z)}^{b(z)} f(x, z) dx \quad (\text{A.6})$$

Consider the following expression

$$\frac{d}{dt} \int_{r=R}^{r=S} (C_A - C_S) r^2 dr = \frac{d}{dt} \int_{y=R^3/3}^{y=S^3/3} (C_A - C_S) dy \quad (A.7)$$

Applying Leibnitz's Rule

$$\frac{d}{dt} \int_{y=R^3/3}^{y=S^3/3} (C_A - C_S) dy = \int_{y=R^3/3}^{y=S^3/3} \frac{\partial}{\partial t} (C_A - C_S) dy - (C_W - C_S) R^2 \dot{R} \quad (A.8)$$

Reverting to the original coordinates

$$\frac{d}{dt} \int_{r=R}^{r=S} (C_A - C_S) r^2 dr + \int_R^S \frac{\partial C_S}{\partial t} r^2 dr = \int_R^S r^2 \frac{\partial C_A}{\partial t} dr + (C_S - C_W) R^2 \dot{R} \quad (A.9)$$

Comparing equation (A.9) to equation (A.3) we get

$$\frac{d}{dt} \int_{r=R}^{r=S} (C_A - C_S) r^2 dr + \int_R^S \frac{\partial C_S}{\partial t} r^2 dr = -DR^2 \left(\frac{\partial C_A}{\partial r} \right) \Big|_{r=R} \quad (A.10)$$

APPENDIX B

MATHEMATICA FILE

(* This program evaluates the radius and concentration profile for a thick shell *)

(* APPROXIMATE METHOD *)

Needs["Graphics`Legend`"]

\$TextStyle = {FontFamily → "Times", FontSize → 15};

$\rho = 1000$;

$K_h = 0.639 \cdot 10^{-9}$;

$\text{Gascon} = 8314./30$;

$T = 300.$;

$P_a = 1 \cdot 10^5$;

$A = \text{Gascon} \cdot T$; (* $A = R_g \cdot T$ *)

$R_0 = 1/10^6$; (* initial critical radius *)

$C_2 = 10^8$; (* indicative of the size of the shell *)

$S = (1 + C_2)^{(1/3)}$; (* Size of the liquid shell in N-D form *)

$C_3 = 0.4$; (* Slightly varying with C_3 decreases R with increasing C_3 *)

$C_4 = 100$; (* Zero variation with C_4 *)

$C_5 = (\rho \cdot A)/P_a$;

$C_6 = K_h \cdot P_a$;

$C_7 = 6 \cdot \rho^2 \cdot K_h^2 \cdot (\text{Gascon} \cdot T)^2$;

$P_f = P_a/10^5$; (* P_f is related to P_a , cannot change individually *)

$P_g = 10$; (* initial gas Pressure in N-D form *)

$$C0=Kh*Pg*10^5;$$

$$(* \zeta = \varepsilon^2 *) (* X[t] = \zeta *)$$

$$(* \text{Definition of } M *)$$

$$M = (3*\rho*R0^3)/(S-R[t])^2*(S^5/30-(S^2*R[t]^3)/3+(S*R[t]^4)/2-R[t]^5/5);$$

$$(* \text{Mass Balance/Diffusion Equation} *)$$

$$\text{Term1}=(Pa*R0^3*\text{Sqrt}[X[t]]/(A*(M-\rho*R0^3*(S^3-R[t]^3)));$$

$$\text{Term2}=(M*Kh*Pa)*(1+\text{Sqrt}[X[t]]/(R[t]^3*(M-\rho*R0^3*(S^3-R[t]^3)));$$

$$\text{Term3}=-(\rho*Kh*Pa*R0^3)*(S^3-R[t]^3)/(M-\rho*R0^3*(S^3-R[t]^3));$$

$$\text{Term4}=-C6*(1+(\text{Sqrt}[X[t]])/R[t]^3);$$

$$f1=2*\text{Sqrt}[X[t]]*(6*C4*C5)*(R[t]^2/(S-R[t]))*(\text{Term1}+\text{Term2}+\text{Term3}+\text{Term4});$$

$$(* \text{Momentum equation} *)$$

$$f2 = (1+C2)/(4*(C2+1-R[t]^3))*(((\text{Sqrt}[X[t]]+1)*Pg)/(R[t]^2)-Pf*R[t]-C3);$$

$$\text{sol1} = \text{NDSolve}[\{\text{Derivative}[1][X][t] == f1, \text{Derivative}[1][R][t] == f2, R[0] == 1.0, X[0] == 0.000001\}, \{X[t], R[t]\}, \{t, 0, 10000\}];$$

$$Cwall1 = ((\text{Sqrt}[\text{Evaluate}[\{X[t]\}/.\text{sol1}]]+1)*(Pg*10^5*Kh))/\text{Evaluate}[\{R[t]\}/.\text{sol1}]^3 ;$$

$$\text{Pressure}=((1+\text{Sqrt}[\text{Evaluate}[\{X[t]\}/.\text{sol1}]]*Pg)/(\text{Evaluate}[\{R[t]\}/.\text{sol1}]^3);$$

$$(* \text{All three equations} *)$$

$$(* \text{This method uses the momentum + interfacial diffusion + overall mass balance} *)$$

$$Mdash = (3*\rho)/(S-R[t])^2*(S^5/30-(S^2*R[t]^3)/3+(S*R[t]^4)/2-R[t]^5/5) ;$$

$$Cwall2 = C0*(1/(Kh*A)+\rho*(S^3-1)+2*((S^3-1)/(S^3-R[t]^3))*(Mdash-\rho*(S^3-R[t]^3)))/(R[t]^3/(Kh*A)+(2*R[t]^3*(Mdash-\rho*(S^3-R[t]^3))/(Kh*A*\rho*(S^3-R[t]^3)))+2*Mdash-\rho*(S^3-R[t]^3)) ;$$

$$f2 = (1+C2)/(4*(C2+1-R[t]^3))*(((\text{Sqrt}[X[t]]+1)*Pg)/(R[t]^2)-Pf*R[t]-C3);$$

```
sol2 = NDSolve[{Derivative[1][X][t] == f1, Derivative[1][R][t] == f2, R[0] == 1.0, X[0] == 0.000001}, {X[t], R[t]}, {t, 0, 10000}];
```

(* This method uses (1) momentum (2) interfacial mass balance (3) Overall mass balance only and no diffusion equation explicitly *)

```
Cwall3 = (Kh*Pa*Pg*(Sqrt[X[t]] + 1))/R[t]^3;
```

```
Y = -2*Cwall3 + (2*C0*(S^3 - 1))/(S^3 - R[t]^3) - (2*Cwall3*R[t]^3)/(Kh*A*ρ*(S^3 - R[t]^3));
```

```
f1 = (12*Sqrt[X[t]]*C4*C5*R[t]^2*Y)/(Pg*(S - R[t]));
```

```
f2 = ((C2 + 1)*(-C3 - Pf*R[t] + ((Sqrt[X[t]] + 1)*Pg)/R[t]^2))/(4*(-R[t]^3 + C2 + 1));
```

```
sol3 = NDSolve[{Derivative[1][X][t] == f1, Derivative[1][R][t] == f2, R[0] == 1., X[0] == 1.0^(-8)}, {X[t], R[t]}, {t, 0, 10000}];
```

(* Infinite medium *)

```
f1 = (2.*C4*C7*(R[t]^3 - Sqrt[X[t]] - 1)^2)/R[t]^2;
```

```
f2 = -(C3/4) - (1/4)*Pf*R[t] + ((Sqrt[X[t]] + 1)*Pg)/(4*R[t]^2);
```

```
sol = NDSolve[{Derivative[1][X][t] == f1, Derivative[1][R][t] == f2, R[0] == 1., X[0] == 0}, {X[t], R[t]}, {t, 0, 10000}];
```

```
Cwall4 = ((Sqrt[Evaluate[{X[t]} /. sol]] + 1)*(Pg*10^5*Kh))/Evaluate[{R[t]} /. sol]^3;
```

```
Pressure = ((1+Sqrt[Evaluate[{X[t]} /. sol]))*Pg)/(Evaluate[{R[t]} /. sol]^3);
```

(* Plotting the concentration and radius profile *)

```
Plot[{Evaluate[{Cwall1} /. sol1], Evaluate[{Cwall2} /. sol2], Evaluate[{Cwall3} /. sol3], Evaluate[{Cwall4} /. sol]}, {t, 0., 40}, PlotStyle → {RGBColor[1, 0, 0], RGBColor[0, 1, 0], RGBColor[0, 0, 1], RGBColor[0, 0, 0]}, PlotRange → {0, 0.0007}, GridLines →
```



```

Automatic, Frame → True, FrameLabel → {"Dimensionless Time ( $t \setminus t_{\text{ref}}$ )",
"Dimensionless Radius ( $R \setminus R_0$ )"}];

Complete = 5.64017003303139 + 0.41736873621895043*t - 0.0005544333726034403*
t^2 + 5.317464912426975*10^(-7)* t^3 - 1.90588641250408*10^(-10)*t^4 ;

Plot[{Evaluate[{R[t]} /. sol1], Evaluate[{R[t]} /. sol2], Evaluate[{R[t]} /. sol3],
Evaluate[{R[t]} /. sol], Complete}, {t, 0, 1200}, PlotStyle → {AbsoluteDashing[{2}],
AbsoluteDashing[{4}], AbsoluteDashing[{8}], AbsoluteDashing[{13}],
AbsoluteDashing[{0}]}], PlotLegend → {"Method 1", "Method 2", "Method 3", "Infinite-
Medium", "Complete"}, LegendPosition → {0.43, -0.50}, LegendShadow → {0, 0},
LegendSize → {0.53, 0.49}, PlotStyle → {Thickness[100]}, PlotRange → {0, 400},
GridLines → Automatic, Frame → True];

```

REFERENCES

- [1] Arefmanesh A., Advani S. G., and Michaelides E. E. An accurate numerical solution for mass diffusion-induced bubble growth in viscous liquids containing limited dissolved gas. *Int. J. Heat Mass Transfer.*, 35: 1711-1722, 1992.
- [2] Amon M. and Denson C. D. A study of the dynamics of foam growth: analysis of the growth of closely spaced spherical bubbles. *Poly. Eng. Sci.*, 24: 1026-1034, 1984.
- [3] Rayleigh Lord. On the pressure developed in a liquid during the collapse of a spherical cavity. *Phil. Mag.*, 6th Ser., 34: 94, 1917.
- [4] Plesset M. S. and Zwick S. A. A non-steady heat diffusion problem with spherical symmetry. *J. Appl. Phys.*, 23: 95-98, 1952.
- [5] Plesset M. S. and Zwick S. A. The growth of vapor bubbles in superheated liquids. *J. Appl. Phys.*, 25: 493-500, 1954.
- [6] Forster H. K. and Zuber N. J. Growth of a vapor bubble in a superheated liquid. *J. Appl. Phys.*, 25: 474-478, 1954.
- [7] Dergarabedian P. the rate of growth of vapor bubbles in superheat water. *J. Appl. Mech.*, 20: 537-545, 1953.
- [8] Birkhoff G., Margulies R. S., and Horning W. A. Spherical bubble growth. *Physics Fluids*, 3: 201-204, 1958.
- [9] Scriven L. E. On the dynamics of phase growth. *Chem. Eng. Sci.*, 10: 1-13, 1959.
- [10] Rosner D. E. and Epstein M. Effect of interface kinetics, capillarity and solute diffusion on bubble growth rates in highly supersaturated liquids. *Chem. Eng. Sci.*, 27: 69-88, 1972.

- [11] Cable M. and Frade J. R. Numerical solution for diffusion-controlled growth of spheres from finite initial size. *J. Mater. Sci.*, 22: 149-154, 1987.
- [12] Cable M. and Frade J. R. Diffusion controlled growth of multi-component gas bubbles. *J. Mater. Sci.*, 22: 919-924, 1987.
- [13] Ward C. A. and Tucker A. S. Thermodynamic theory of diffusion-controlled bubble growth or dissolution and experimental examination of the predictions. *J. Appl. Phys.*, 46: 233-238, 1975.
- [14] Barlow E. J. and Langlois W. E. Diffusion of gas from a liquid into an expanding bubble. *IBM Journal*, 6: 329-337, 1962.
- [15] Langlois W. E. Similarity rules for isothermal bubble growth. *J. Fluid Mech.*, 15: 111-118, 1963.
- [16] Szekely J. and Martins G. P. Non-equilibrium effects in growth of spherical gas bubbles due to solute diffusion. *Chem. Eng. Sci.*, 26: 147-159, 1971.
- [17] Yung C. N., De Witt K. J., Brockwell J. L., Mcquillen J. B., and Chai A. T. A numerical study of parameters affecting gas bubble dissolution. *J. Colloid and Interface Science*, 127: 442-452, 1989.
- [18] Patel R. D. Bubble growth in viscous Newtonian liquid. *Chem. Eng. Sci.*, 35: 2356-2358, 1980.
- [19] Qiu D. M., Dhir V. K., and Chao D. Single-bubble dynamics during pool boiling under low gravity conditions. *J. Thermophys. Heat Transfer.*, 16 (3): 336-345, 2002.
- [20] Prodanovic V., Fraser D., Salcudean M. bubble behavior in sub-cooled flow boiling of water at low pressures and low flow rates. *Int. J. Multiphase Flow.*, 28(1): 1-19, 2002.

- [21] Robinson A. J. and Judd R. D. Bubble growth in a uniform and spatially distributed temperature field. *Int. J. Heat Mass Transfer.*, 44(14): 2699-2710, 2001.
- [22] Miyatake O., Tanaka I., and Lior N. A simple universal equation for bubble growth in pure liquids and binary solutions with a non-volatile solute. *Int. J. Heat Mass Transfer.*, 40(7): 1577-1584, 1997.
- [23] Venerus D. C., Yala N., and Bernstein B. Analysis of diffusion-induced bubble growth in viscoelastic liquids. *J. Non-Newton. Fluid.*, 75 (1): 55-75, 1998.
- [24] Venerus D. C. and Yala N. Transport analysis of diffusion-induced bubble growth and collapse in viscous liquids. *AIChE. J.* 43(11): 2948-2959, 1997.
- [25] Venerus D. C. Diffusion-induced bubble growth in viscous liquids of finite and infinite extent. *Pol. Eng. Sci.*, 41(8): 1390-1398, 2001.
- [26] Han D. C. and Yoo H. J. Studies on Structural Foam Processing. IV. Bubble Growth During Mold Filling. *Pol. Eng. Sci.*, 21(9): 518-533, 1981.
- [27] Barrow G. M. *Physical Chemistry*. McGraw-Hill, New York, 1979.
- [28] Van Wylen G. J. and Sonntag R. E. *Fundamentals of Classical Thermodynamics*. John Wiley & Sons, New York, 1965.
- [29] Schlichting H. *Boundary Layer Theory*. McGraw-Hill, New York, 1978.
- [30] Ozisik M. N. *Heat Conduction*. John Wiley & Sons, New York, 1980.
- [31] Arpaci V. S. and Larsen P. S. *Convection Heat Transfer*. Prentice-Hall, Inc., New Jersey, 1984.

MICHIGAN STATE UNIVERSITY LIBRARIES



3 1293 02470 0076